Review of aeronautical fatigue and structural integrity investigations in the UK during the period April 2019 - April 2021

Hallam, D

DSTL/TR132845 v1
30 June 2021

Dstl
Platform Systems
Porton Down
Salisbury
Wilts
SP4 0JQ

Release Conditions

This document has been compiled by Dstl but contains information released by each author's organisation for presentation to the International Committee on Aeronautical Fatigue and Structural Intergity (ICAF).

Executive summary

This review is a summary of the aeronautical fatigue and structural integrity investigations carried out in the United Kingdom during the period April 2019 to April 2021.

The review has been compiled for the International Committee on Aeronautical Fatigue and Structural Integrity (ICAF) website and 2021 ICAF webinar. Contributions generously provided by colleagues from within the aerospace industry and universities are gratefully acknowledged. The names of contributors and their affiliation are shown below the title of each item.

Table of contents

Executive summary i

1 Introduction 1

2 Developments in fatigue analysis 2

2.1 Probabilistic Fatigue Methodology for Safe-Life Design and Analysis......... 2

2.2 Developments in Fatigue Design Tools 6

2.3 BEASY crack growth software... 11

3 Guidance and fatigue performance of additive manufactured parts 17

3.1 Guidance on the qualification and certification of additive manufactured parts in military aviation... 17

3.2 Fatigue behaviour of aerospace titanium Ti-6Al-4V made of wire based directed energy deposition (w-DED)... 18

4 Enhancing fatigue performance 25

4.1 Laser peening fatigue research – Cranfield University 25

4.2 Crack trajectory modifications and life extension due to laser peening residual stress.. 29

5 Understanding fatigue behaviour 32

5.1 Microstructure-sensitive prognosis of fatigue crack nucleation 32

5.2 Integrated approaches to understand the transition from corrosion to mechanical driven cracks at high temperature 32

6 Non-destructive testing 34

6.1 Development of a protocol for model-assisted qualification (MAQ) of NDT techniques 34

7 Structural health monitoring 35

7.1 Development of a Wireless Acoustic Emission Monitoring System for Aerospace... 35

7.2 Structural Health Monitoring, Manufacturing and Repair Technologies for Life Management Of Composite Fuselage - SHERLOC 38

7.3 Galvanic Corrosion Sensors.. 41

8 Advanced repair and coating technologies 44

8.1 Optimal Control of Resin Injection Repair for Composite Laminates 44

8.2 De-icing using icephobic coatings alongside thermal de-icing systems 47

9 Advanced composite materials and structural design approaches 49

9.1 Multi-functional Shape Memory Alloy Tufted Composite Joints 49

9.2 Advanced Design of Composite Structures for Future Combat Aircraft 51

Initial distribution 52

Report documentation page v5.0 53

1 Introduction

This review is a summary of the aeronautical fatigue and structural integrity investigations carried out in the United Kingdom during the period April 2019 to April 2021.

The review has been compiled for the International Committee on Aeronautical Fatigue and Structural Integrity (ICAF) website and the 2021 ICAF webinar.

The contributions generously provided by colleagues from within the aerospace industry and universities are gratefully acknowledged. The names of contributors and their affiliation are shown below the title of each item.

The format of the paper is similar to that of recent UK ICAF reviews; the topics covered include:

- Developments in fatigue analysis
- Guidance and fatigue performance of additive manufactured parts
- Enhancing fatigue performance
- Understanding fatigue behaviour
- Non-destructive testing
- Structural health monitoring
- Advanced repair and coating technologies
- Advanced composite materials and structural design approaches

References are annotated at the end of each contribution and are self-contained within the contribution. Figure and table numbers are also self-contained within the contribution.

2 Developments in fatigue analysis

2.1 Probabilistic Fatigue Methodology for Safe-Life Design and Analysis

Joshua Hoole[1], Pia Sartor[1], Julian Booker[1], Jonathan Cooper[1], Xenofon V. Gogouvitis[2], Amine Ghouali[3] and R. Kyle Schmidt[4]
[1]Faculty of Engineering, University of Bristol, United Kingdom, email: jh12317@bristol.ac.uk
[2]Safran Landing Systems, Gloucester, United Kingdom
[3]Safran Landing Systems, Vélizy, France
[4]Safran Landing Systems, Ajax, ON, Canada

2.1.1 Background

Aircraft landing gear and other safety-critical aerospace structures continue to be designed and certified using a ‘safe-life’ approach [1]. To prevent fatigue crack initiation, classical stress-life (S-N) and strain-life analysis methods supported by full-scale testing, are used to determine the safe-life at which a component must be retired from service [1]. However, the engineering parameters relating to the fatigue design of such components, including material properties and in-service loading, demonstrate significant variability. This variability is currently mitigated using design conservatism, which can ultimately lead to over-weight components, or components which do not fully exploit their potential useful life [2].

Probabilistic methodologies have been proposed as a route to better representing the inherent variability of fatigue design parameters within analysis methods [3]. Probabilistic methodologies represent the variability in engineering parameters using probability distributions (e.g. Normal, Weibull, etc.) and using various approaches, such as Monte Carlo Simulation (MCS), propagate the variability through the existing fatigue analysis method to the analysis output (e.g. the fatigue damage estimated from Miner’s rule) [3].

However, there are a number of inhibiting factors that prevent the wider adoption of probabilistic approaches within industrial environments, including limited data availability along with the resources and technical knowledge required to implement probabilistic methods [4, 5].

This project focused on developing a probabilistic fatigue methodology for safe-life landing gear components that aimed to ease the future adoption of probabilistic approaches within engineering design and assessment.

This work was undertaken as a collaboration between the University of Bristol and Safran Landing Systems during the “Large Landing Gear of the Future Project” (LLGF) funded by the Aerospace Technology Institute (Grant No. 113077). The publications disseminated during this project are included within the references list of this project summary and are highlighted with an asterisk ‘*’.

2.1.2 Developed Methodology

A probabilistic fatigue methodology was developed for safe-life components and an overview is shown in Figure 1. Within the LLGF project, the methodology was demonstrated on case studies using components that were representative of typical aircraft landing gear components. The methodology employed an MCS approach coupled with a classical Stress-Strength Interference (SSI) method to reduce the computational expense of a ‘pure’ MCS [5, 6]. Within each iteration of the MCS, the material properties, geometry and in-service load spectrum for a complete design safe-life were statistically simulated. Repeated iterations of the MCS permitted the resulting variability in the accumulated fatigue damage predicted from Miner’s rule to be estimated at various fatigue ‘hot-spots’ across the component as shown in Figure 1. When coupled with robust statistical characterisation methods for SSI, fatigue reliability estimates could then be computed at a feature/hot-spot, component and assembly level. The use of an MCS approach also permitted the entire complexity of the existing S-N fatigue analysis process to be retained. Consequently, surrogate modelling methods had to be used to replace the computationally intensive finite element load and stress models that are commonly used in modern fatigue analysis approaches [7].

Whilst significant work has previously been performed concerning probabilistic approaches to safe-life fatigue analysis [3], the recent introduction of ‘big-data’ sources has significantly reduced the challenge of data availability within probabilistic approaches to fatigue design [8]. A highlight of this project was the exploitation of real-time aircraft tracking from transponder data using Flightradar24® [9]. Within this work, algorithms were developed to identify and characterise the ground manoeuvres performed by in-service aircraft based on fleet-wide transponder data. From processing the transponder data, approximately 30 individual statistics relating to aircraft ground manoeuvre occurrence and sequencing could be constructed, including some statistical measures that have not previously been captured within traditional aircraft load monitoring campaigns [9]. Such data and statistics are vital elements in the construction of load spectra within landing gear fatigue design. As highlighted in Figure 1, the exploitation of real-time aircraft tracking data also provided the required information to characterise the variability in aircraft ground manoeuvres, facilitating the statistical simulation of landing gear load spectra within the probabilistic fatigue methodology.

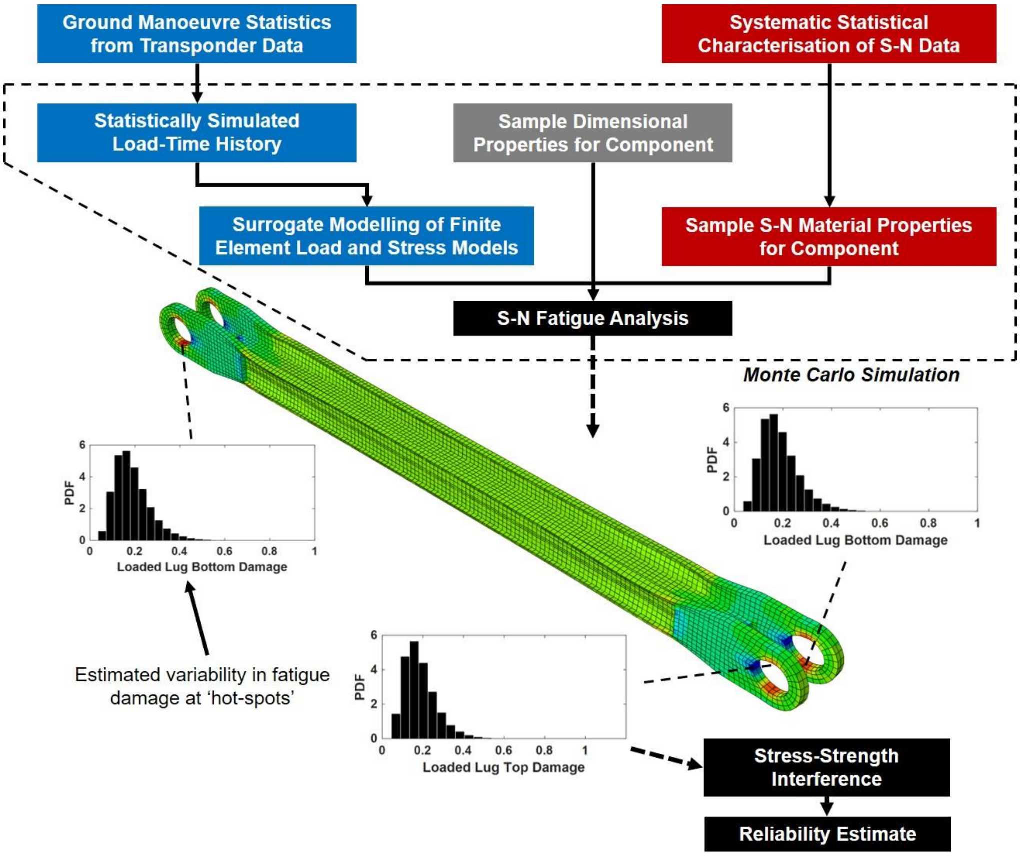

Figure 1: A flowchart overview of the probabilistic fatigue methodology applied to a landing gear component (3D model created in ABAQUS®).

Beyond the adoption of novel data sources, elements of the probabilistic fatigue methodology also aimed to facilitate the wider adoption of probabilistic methodologies in engineering design, analysis, and assessment:

- **Systematic and Robust Statistical Characterisation Process [10]:** Practicing engineers do not typically have a strong statistical background [4] and consequently, a systematic statistical characterisation process is required to support the down-selection of probability distribution types within a probabilistic approach. The systematic statistical characterisation process was demonstrated on a typical S-N dataset [11]. The employment of the process permitted a challenge of the routinely assumed distribution types for fatigue life through the selection of the 3-Parameter Weibull distribution, resulting in an increase in the estimated safe-life for a benchmark component.

- **Implementation Framework [5]:** One of the significant challenges relating to the adoption of probabilistic approaches is the additional technical knowledge and resources required to implement such an approach. In order to reduce this resource burden, a probabilistic methodology framework was developed to demonstrate how the techniques required for a probabilistic approach could be used to support optimisation-based design, digital-twins and the further exploitation of 'big-data' sources.

2.1.3 Future Work

Whilst the probabilistic fatigue methodology and framework were found to overcome a majority of the factors that currently inhibit the wider adoption of probabilistic methods within the engineering sector, the application of the methodology to a range of case studies also highlighted a remaining challenge regarding the implementation of probabilistic approaches. Whilst a probabilistic methodology permitted the fatigue reliability of a feature, component or assembly to be estimated, probabilistic design and acceptance criteria (i.e. reliability targets) are yet to be defined within the aerospace fatigue design community. Work performed as part of this project details potential routes to defining reliability targets for aerospace components [5].

It is anticipated that big-data sources will continue to provide new opportunities within the field of aerospace fatigue design and assessment. Therefore, it is hoped that the work performed during this project concerning the use of real-time tracking of in-service aircraft [9] has demonstrated the potential utility and extensibility of such data sources within this field and the wider aerospace sector.

References

[1] Hoole J., Sartor, P. and Cooper, J. E., "Safe-Life Fatigue and Sensitivity Analysis: A Pathway Towards Embracing Uncertainty?", *Proceedings of the Royal Aeronautical Society 5th Aircraft Structural Design Conference,* Manchester, U.K., October, 2016.

[2] * Hoole J., Sartor, P., Booker, J. D., Cooper, J. E., Gogouvitis, X. V. and Schmidt, R. K., "Evaluating the Impact of Conservatism in Industrial Fatigue Analysis of Life-Limited Components", *Proceedings of the 12th International Fatigue Congress (Fatigue 2018)*, Poitiers, France, May, 2018.

[3] Ocampo, J., Millwater, H., Singh, G., Smith, H., Abali, F., Nuss, M., Reyer, M. and Shiao, M., "Development of a Probabilistic Linear Damage Methodology for Small Aircraft", *Journal of Aircraft*, **48**, (6), 2090-2106, 2011.

[4] Goh, Y. M., McMahon, C. A. and Booker, J. D., "Improved utility and application of probabilistic methods for reliable mechanical design", *Proceedings of the Institution of Mechanical Engineers, Part O: Journal of Risk and Reliability*, **223**, (3), 199-213, 2009.

[5] * Hoole J., Sartor, P., Booker, J. D., Cooper, J. E., Gogouvitis, X. V., Ghouali, A. and Schmidt, R. K., "A Framework to Implement Probabilistic Design of Safe-Life Components" in *ICAF 2019 – Structural Integrity in the Age of Additive Manufacturing* (Eds. A. Niepokolczycki and J. Komorowski), Springer, 2019.

[6] * Hoole J., Sartor, P., Booker, J. D., Cooper, J. E., Gogouvitis, X. V. and Schmidt, R. K., "Probability Distribution Type for the Accumulated Fatigue Damage from Miner's Rule in Fatigue Design", in *Mechanical Fatigue of Metals – Experimental and Simulation Perspectives* (Eds. J. A. F. O. Correia, A. M. P. De Jesus, A. A. Fernades and R. Calçada), Springer, 2009.

[7] * Hoole J., Sartor, P., Booker, J. D., Cooper, J. E., Gogouvitis, X. V. and Schmidt, R. K., "Comparison of Surrogate Modeling Methods for Finite Element Analysis of Landing Gear Loads", *Proceedings of AIAA SciTech2020*, Orlando, Florida, U.S.A., January, 2020.

[8] Graham, K., Artim, M. and Daverschot, D., "Aircraft Fatigue Analysis in the Digital Age", *Proceedings of the International Committee on Aeronautical Fatigue and Structural Integrity (ICAF) 36th Conference and 29th Symposium*, Nagoya, Japan, June, 2017.

[9] * Hoole J., Sartor, P., Booker, J. D., Cooper, J. E., Gogouvitis, X. V. and Schmidt, R. K., "Landing Gear Ground Manoeuvre Statistics from Automatic Dependent Surveillance-Broadcast Transponder Data", *Under Preparation,* 2021.

[10] * Hoole J., Sartor, P., Booker, J. D., Cooper, J. E., Gogouvitis, X. V. and Schmidt, R. K., "Systematic statistical characterisation of stress-life datasets using 3-Parameter distributions", *International Journal of Fatigue*, **129**, 2019.

[11] IHS ESDU, "Endurance of high-strength steels", *ESDU 04019*, 2006.

2.2 Developments in Fatigue Design Tools

A. Halfpenny, R. Plaskitt - HBM Prenscia

2.2.1 Developments in fatigue analysis

2.2.1.1 General Developments

HBM Prenscia continue to develop their material fatigue testing capabilities and the fatigue damage models used in their nCode software products for fatigue and durability analysis.

- nCode DesignLife, for fatigue analysis from finite element analysis stress results, has been developed to support:
    - Fatigue damage models for new joints and bonding methods, particularly thin sheet welded joints, with corresponding fatigue testing procedures and characterisation to derive fatigue curves for the joint and loading.
    - The bearing bypass (aka stress severity factor) method for fatigue calculation of joints, as described by Niu in “Airframe Structural Design”. This considers the bearing and the bypass loads, with the bearing load transferred through a fastener from one sheet to connected sheets. The peak stress, for fatigue analysis, is the sum of the contribution of the bearing stress and the bypass stress.
    - The four-parameter Weibull equation for Safe and mean S-N curves defined in UK Defence Standard 00-970 Design and Airworthiness Requirements for Service Aircraft.
    - The Brown-Miller multi-axial fatigue damage model and the Walker mean stress correction method.
- The Advanced Materials Characterisation & Test laboratory (AMCT) has completed some relevant and publicly presented fatigue testing. This includes:
    - Strain-controlled fatigue testing to characterise surface treatment effects in landing gear materials. This work is with Select Engineering Services (USA), General Atomics (USA) and USAF 417th Landing Gear Office. It is described in an ASIP 2019 technical paper and presentation, and is summarised in this review with the abstract, materials and process selection, and conclusions.

2.2.1.2 Surface Treatment Effects in Fatigue Analysis of Landing Gear Materials (ASIP 2019, December 2-5, 2019, San Antonio, TX)

B. Griffiths[1] PE., A. Halfpenny[2] PhD., B. Madsen[3], M. Hill[2] PhD., M. Chelu[2], A. Clark[4]
[1]Select Engineering Services; [2]HBM Prenscia; [3]General Atomics Systems Integration;
[4]USAF 417 SCMS/GUEA, Landing Gear Systems

The presentation and paper can be downloaded from:

- http://meetingdata.utcdayton.com/Agenda/asip/2019/agenda.html
- Session 10: Characterization, Modeling & Testing III

Abstract

As of October 2018, the average age of aircraft across the entire United States Air Force (USAF) fleet was 28 years, with some specific aircraft averaging as much as 56 years. Many of these aircraft have been maintained well beyond their original design life. Landing gear undergo surface treatments to protect them against the environment and control their dimensionality. Many USAF landing gear components currently in service have been overhauled or re-worked numerous times. The effect of these processes on fatigue life was not considered in legacy designs.

This paper describes an efficient manner for developing a database of material and surface treatment fatigue properties. The approach is based on a combination of Strain-life (EN) fatigue testing and Surface Finish Factors. The paper describes the method in detail and presents conclusions for the first three materials and their associated surface conditions. It concludes by presenting a Finite Element Analysis of a typical landing gear and quantifying the effect of surface treatments on the fatigue life.

Positive conclusions resulting from this work include: increased confidence in life extension for aging aircraft landing gear components, the timely removal of landing gear components from service to decrease the risk of failure, and the potential for improvements to repetitive overhaul processes to reduce their negative impact on fatigue life.

Materials and Process Selection

A comprehensive review of landing gear materials and processes was conducted in order to identify, prioritize, and select material/process combinations for testing. Table 1 gives a list of the identified USAF landing gear materials and Table 2 gives a list of associated coating, manufacturing, and overhaul processes.

Table 1: List of Identified Materials Used in USAF Landing Gears

	Steel		Aluminum		Stainless Steel	Titanium
300M	4340	4330V Mod	7075	7049	17-4 PH	Ti-6Al-4V
4140	4130	8630	7175	7050	PH 13-8Mo	Ti-10V-2Fe-3Al
8740	Ferrium S53	Aermet 100	2024	2014		
HP 9-4-30	Ferrium M54	AF 1410	7085			

Table 2: List of USAF Landing Gear Coating, Manufacturing, and Overhaul Processes

Coatings	Ancillary Processes
Chrome Electroplating	Grinding/Machining
Cadmium Electroplating	Abrasive Blasting
Anodizing	Temper Etching
Electroless Nickel Plating	Chemical/Electrolytic Cleaning and Stripping
LHE Zinc-Nickel Electroplating	Hydrogen Embrittlement Baking
Tungsten Carbide HVOF Coating	Shot Peening
Electrolytic Nickel Plating	Anodic Etching
Chemical Passivation and Conversion	Acid Pickling

Based on the review, three common materials were selected for testing in this project phase. Two coating processes, chrome plating and anodizing, were also selected with three combinations of application parameters for each process. Nearly all of the ancillary processes were used in the procedures for one or both of the selected coating processes.

The number of potential permutations from the lists in Tables 1 and 2 is substantial. Considerations for repetitive processing further increases the scope of potential test variables. As a result, it is essential to select boundaries that lead to the most meaningful test results. The primary focus of this research is to match the processes/procedures used by the depot overhaul facility at Hill Air Force Base (HAFB). The HAFB overhaul facility uses standards (e.g., MIL, AMS, ASTM) as a basis for all coating, manufacturing, and overhaul processes but also has specific procedures that further dictate processing parameters. These HAFB specific procedures were implemented to the greatest extent possible in all specimen processing.

Surface Treatment Effects (Figure 9 / Slide 14)

- Modify (shift) the baseline curve using K factors – the K_{sur} method:
- Surface treatment effect quantified by a single parameter instead of deriving a new/independent 5-parameter curve.
- Reduced number of tests required to characterize the surface treatment.
- Allows statistical comparisons.
- Different surface treatments on the same material.
- Same surface treatment on different materials.
- Assumes that surface treatment effects are greater at higher cycles.

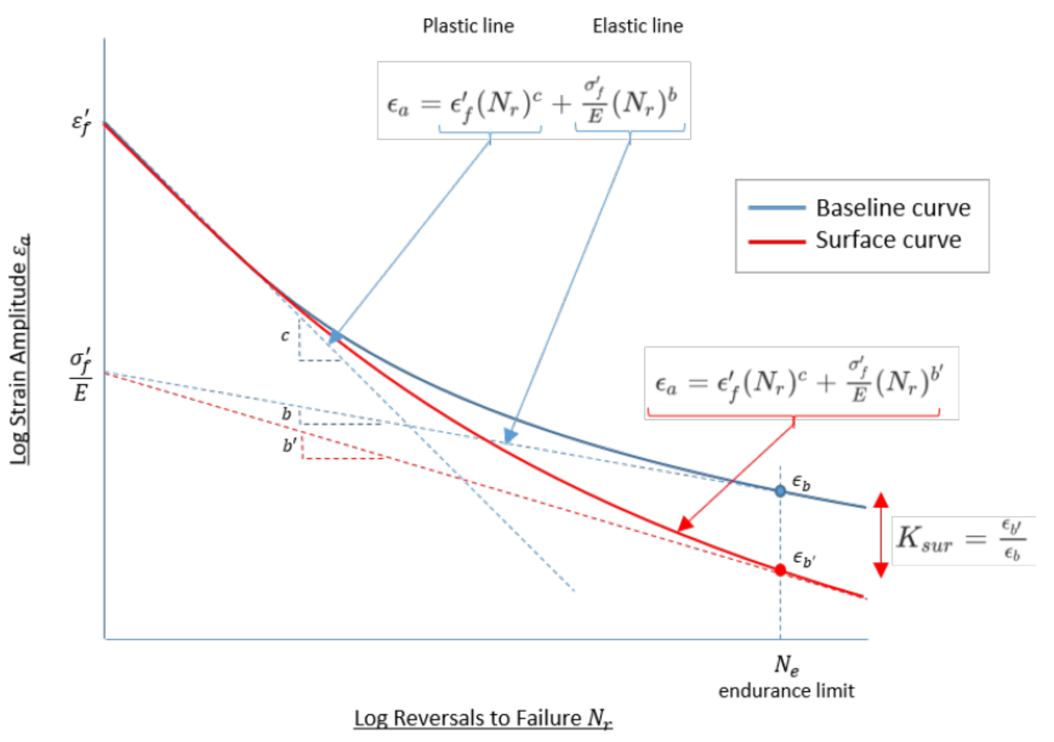

Figure 9: Illustration of the K_{sur} method

Conclusions

Initial material tests show that surface treatments can have a significant effect on high-cycle fatigue.

Three common landing gear materials were selected for testing in this project phase. Two coating processes, chrome plating and anodizing, were also selected with three combinations of application parameters for each process. Nearly all of the ancillary processes listed in Table 2 were used in the procedures for one or both of the selected coating processes.

Tests show that the K_{sur} model, when applied to Strain-life (EN) fatigue data, appears to offer an acceptable fit to the measured data for the materials and surface treatments tested so far. This allows for a reduction in test sample size which leads to more efficient testing. Furthermore, K_{sur} factors can be used in statistical analyses to represent a combined material/surface treatment design curve with a specified reliability and confidence.

Test results have led to the following conclusions that are specifically relevant to the selected materials and surface treatment parameters:

1. Chrome Plating of steel (or anodizing of aluminum) has a significant and adverse effect on the high-cycle fatigue performance of the material. However, its effect on low-cycle fatigue performance is much less. The K_{sur} model offers good correlation with the phenomenon.

2. Shot-peening prior to Chrome Plating (or anodizing) appears to negate completely the detrimental effects of the process.

3. Repetitive surface treatment applications appear to contribute to the statistical scatter, but do not adversely affect the mean fatigue behavior.

Used correctly, the K_{sur} parameters can be combined in order to investigate the effects of multiple surface treatments. A knowledge-base is currently being developed by SES.

Work is continuing to consider more materials, surface treatments, coating depths, the effect of re-applications, etc. However, the K_{sur} parameters are often transferable between similar materials with similar surface treatments. This allows useful design insights to be made by the USAF even before the knowledge-base is fully completed.

Positive outcomes/conclusions resulting from completed surface treatment research and analysis include:

1. Increased confidence in life extension for aging aircraft landing gear components

2. The timely removal of landing gear components from service to decrease the risk of failure

3. The potential for improvements to repetitive overhaul processes that will reduce their negative impact on fatigue life

As USAF or other industries consider extending service life of products these processes must be accounted for. SES now has a road-map to provide testing and data for customers that desire specific material/process treatments.

2.3 BEASY crack growth software

T. Froom, S. Mellings - BEASY

2.3.1 BEASY crack growth capability developments

Over the last few years BEASY have been working on a major redesign of the crack growth simulation software. The new structure preserves the previous crack growth tools, but has been implemented to enable a number of additional crack growth simulation features to be introduced:

- Cracks being able to automatically fully break through part of a structure
- Cracks that can be split at a new external surface, automatically generating multiple crack fronts
- Cracks that can be split across multiple zones, valuably reducing simulation time
- Flexibility to incorporate additional cracks into the model part way through a crack growth simulation

The BEASY crack growth wizard is used to add cracks to BEASY models, and has been further enhanced to also provide new crack initiation and orientation tools as illustrated in Figure 1.

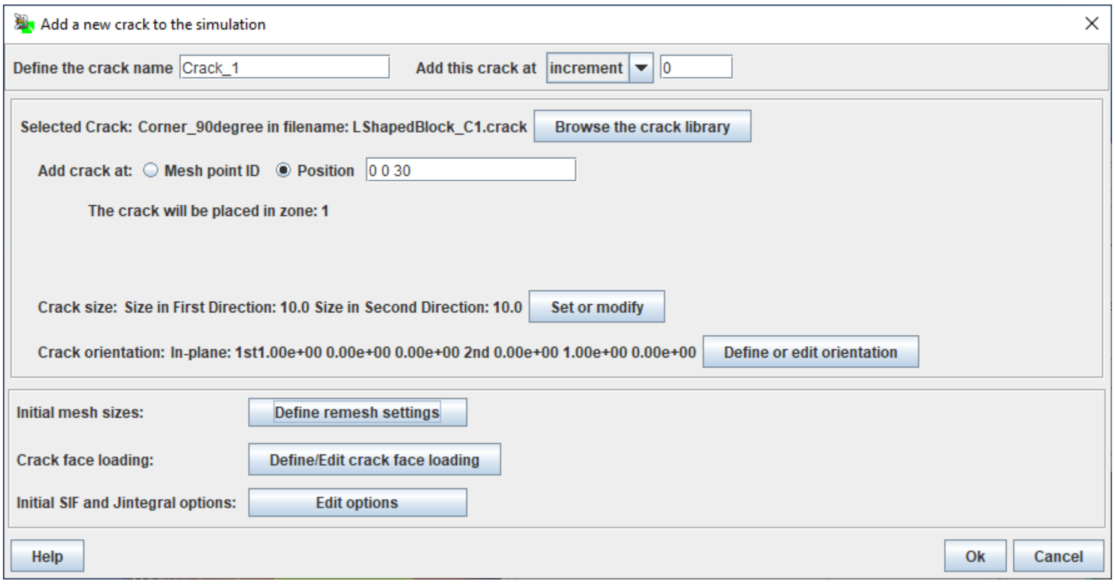

Figure 1: Define a new crack: Finished crack settings

A further feature has been developed allowing users to grow cracks initially using small crack growth increments, and then increasing the growth distance during later crack growth increments; this is used to improve the stability of a crack growth and to enable additional precision to be achieved during the important initial crack growth stages.

2.3.2 Automatic splitting of a crack front

Figure 2 shows the growth sequence of a corner crack as it progresses through an L-shaped bracket.

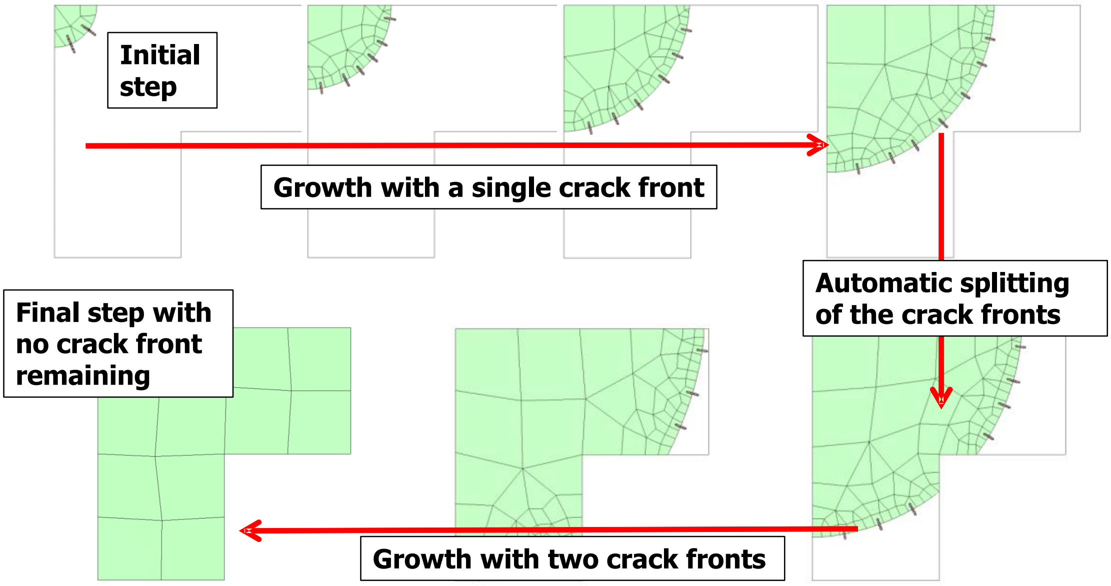

Figure 2: Automatic splitting of a corner crack

In the new BEASY crack growth process, cracks are now simulated as single cracks but allowing for independent crack fronts (two in the case shown above). This process incorporates interaction of the stresses and resultant stress intensity factor (SIF) values for each individual front.

This feature is useful for cracks growing through pipes where a crack can grow through a wall thickness with the crack growing on as a two-bay crack as shown in Figure 3. If this is used in leak before break scenarios, if pressure loading is applied to crack faces, BEASY allows that pressure to be reduced when the crack breaks through the part.

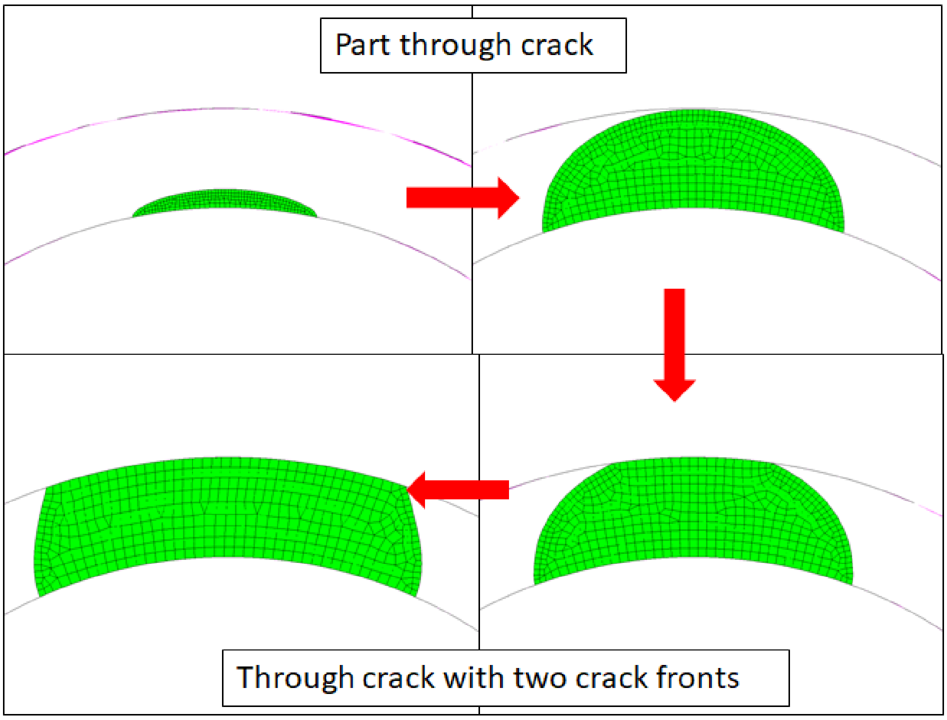

Figure 3: Inner crack breaking through a thin walled pipe

This capability is not limited to just two crack fronts. Figure 4 shows the growth of an embedded crack which splits to create 4 crack fronts.

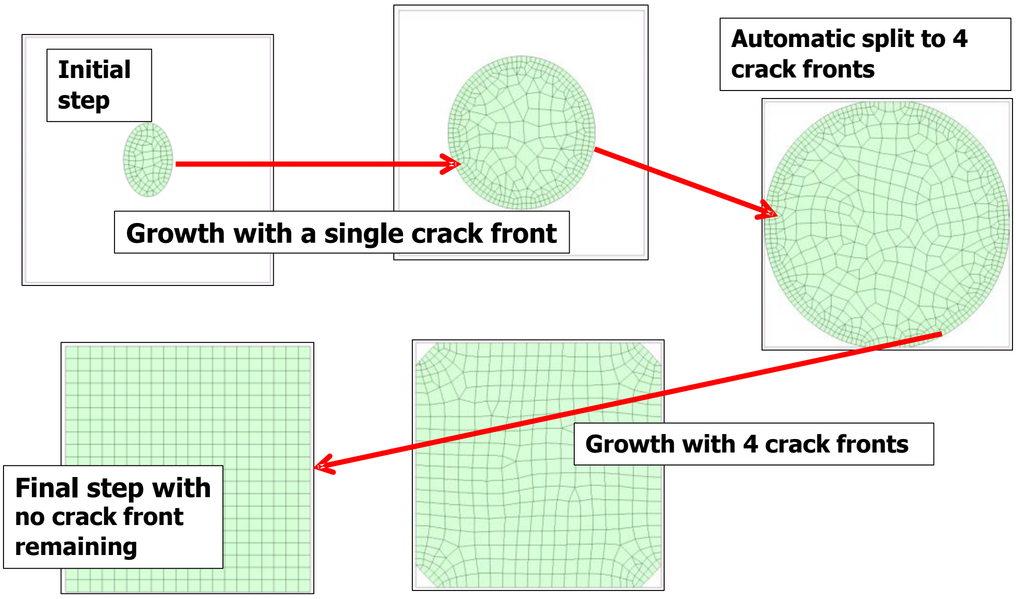

Figure 4: Automatic splitting of an embedded crack

This development allows parts of a crack to fully grow through a section. Figure 5 illustrates an example where an initial corner crack has grown through a section and split to generate two crack fronts and then, as shown in the right hand image part of this crack has fully broken through the upper segment. Crack growth will automatically continue with the remaining crack front.

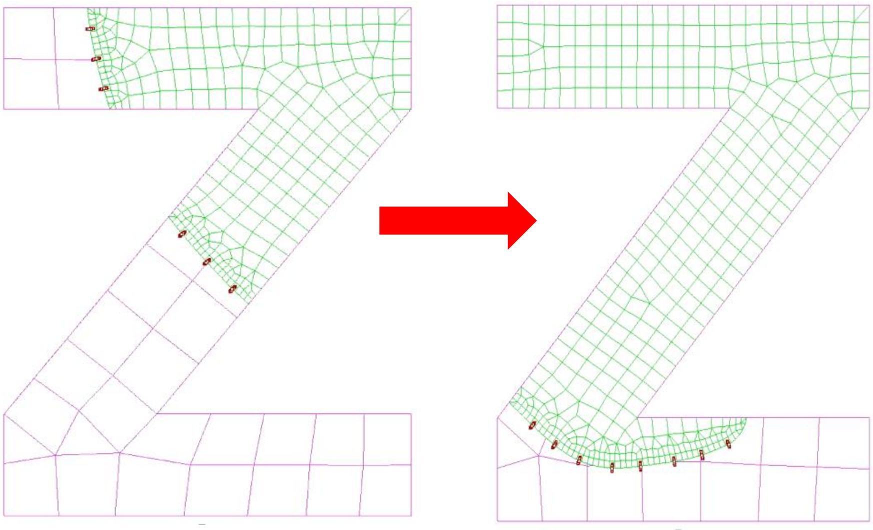

Figure 5: Corner crack through a "Z" specimen

2.3.3 Multiple cracks joining

The new version also allows automatic merging of neighbouring co-planar cracks. In this case the two cracks shown in Figure 6 are growing from an idealised corrosion pit. These cracks grow and automatically coalesce into a single crack.

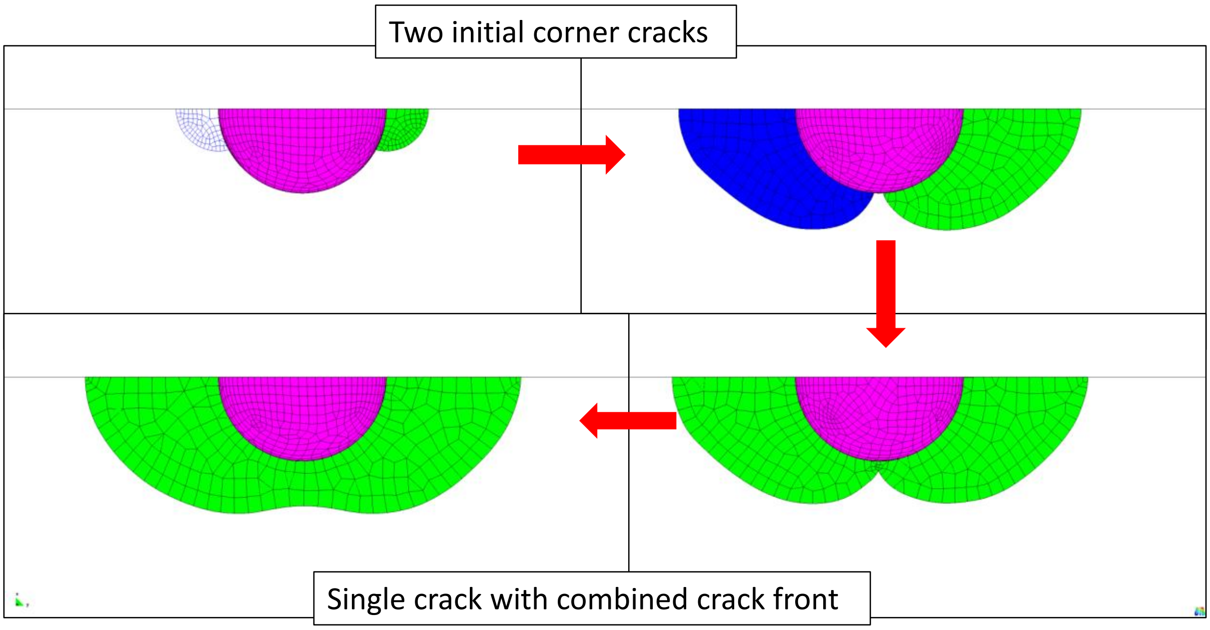

Figure 6: Coplanar cracks automatically joining

This automatic capability is limited to cracks remaining planar when they re-join. However, even where the situation involves non planar cracks joining, this can nevertheless be addressed in BEASY by creating a new custom crack which would allow continuation of the crack growth with the merged crack shape.

2.3.4 Cracks splitting and re-joining

During a crack growth, it is possible for a crack to split, generating two crack fronts but then later re-joining. This feature could be of particular use when evaluating the effects of voids arising, for example, from manufacturing processes or when considering corrosion pitting. Figure 7 shows a corner crack that has grown and been automatically split by an internal cavity. As the crack grows the two crack fronts will eventually automatically re-join. Again this is limited to cracks remaining planar when they re-join, however a custom crack could still be used for non planar cracks.

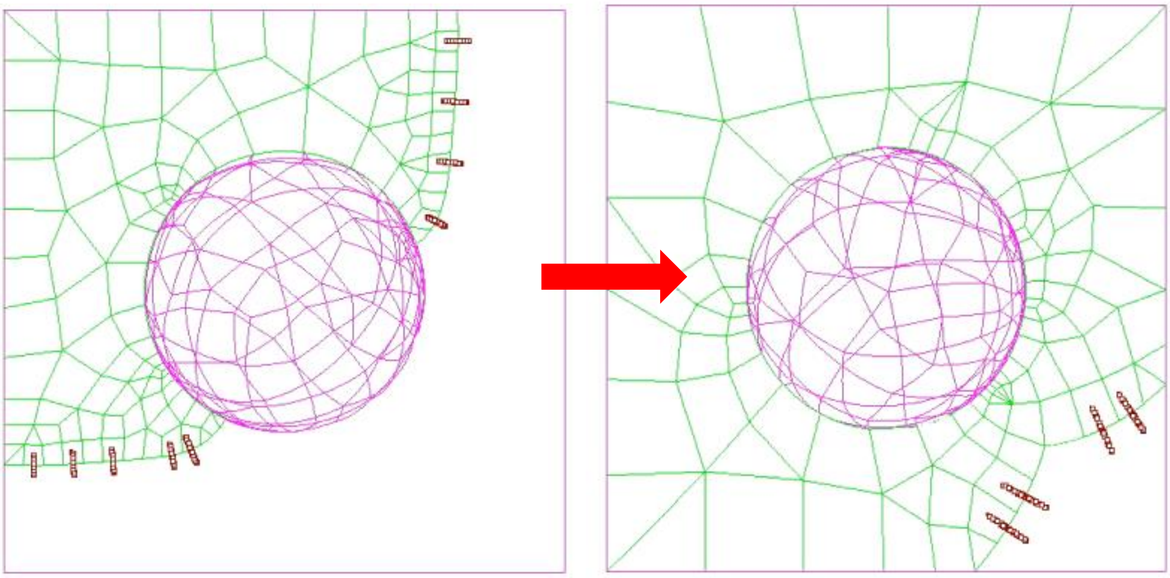

Figure 7: Corner crack split by an internal cavity

2.3.5 Custom cracks

The process of creating custom cracks has been simplified; removing the need to define the crack edge and the crack front in a crack surface. This allows cracks to be defined using a mesh defining the crack surface only.

2.3.5.1 Enhancements when using FE models

Various improvements have been implemented in the BEASY FE interfaces. These tools, used to create BEASY models from existing FE meshes and results, can now create a multiple-load case BEASY model using multiple FE result files (previously BEASY models could only be created using a single FE result file). Many users have their FE results in independent FE result files; this previously required multiple-passes through the BEASY model creation tool. The processes have been simplified, thereby allowing a single pass creation of the BEASY model, which both reduces user time and avoids the risk of errors in manual manipulation of files.

In addition to this:

- The required time for processing large FE models has been reduced
- There have been improvements in the BEASY model cutting feature that improves the creation of a BEASY sub-model, while also simplifying the creation of multiple BEASY zones

3 Guidance and fatigue performance of additive manufactured parts

3.1 Guidance on the qualification and certification of additive manufactured parts in military aviation

D. Fletcher[1], M. Lunt[1], R. Mangham[1], A. Mew[2],
[1]Defence Science and Technology Laboratory (Dstl)
[2]QinetiQ

After the development of guidance material for the qualification and certification of metal additive manufactured parts in military aviation, the Military Aircraft Structural Airworthiness Advisory Group has initiated the expansion of MASAAG paper 124 to also include guidance on polymer components and aircraft systems. As before the aim is to focus on Grade A parts and a working group will be used to contribute knowledge and to peer review the final document. The current version of the guidance is published on the UK Government Website as MASAAG Paper 124:

https://assets.publishing.service.gov.uk/government/uploads/system/uploads/attachment_data/file/920523/MASAAG_Paper_124.pdf.

When complete the second version of the document will also be available on the www.gov.uk website.

3.2 Fatigue behaviour of aerospace titanium Ti-6Al-4V made of wire based directed energy deposition (w-DED)

AK Syed[1], X Zhang[1], ME Fitzpatrick[1], Rob Plaskitt[2], Michelle Hill[2]
[1]Coventry University
[2]HBM Prenscia, UK

3.2.1 NEWAM programme

The work reported here is a part of the New Wire Additive Manufacturing (NEWAM) research programme funded by the UK EPSRC Research Council (Grant No. EP/R027218/1), comprising four UK universities, and supported by 19 industrial partners mainly from the aerospace industry.

Four universities (Cranfield U., U. of Manchester, U. of Strathclyde and Coventry U.) have joined forces to deliver an ambitious research programme over five years with EPSRC funding, and considerable industry support from AM equipment supply chain, service providers and end users.

This NEWAM research programme is focused on the process, material and structural integrity of AM parts, with research areas in:

- Process development
- Process modelling
- Process monitoring
- Non-destructive testing
- Material development
- Material modelling
- Material performance
- Structural integrity

Work at this reporting period has focussed on the aerospace titanium alloy Ti-6Al-4V (Ti64) produced by Wire + Arc Additive Manufacturing (WAAM), which is a Directed Energy Deposition AM process. Specimens were manufactured by Cranfield University's Welding Engineering and Laser Processing Centre. The Coventry University team leads the "Material Performance and Structural Integrity" of NEWAM, determining structural integrity through:

- fatigue initiation - defects, defect tolerance, testing & characterization and modelling
- fatigue fracture - testing & characterisation, crack growth and fracture mechanics
- residual stress - modelling, contour & diffraction test methods, and residual stress intensity

The HBM Prenscia contribution includes strain controlled fatigue testing, for three different materials, in vertical and horizontal build directions. Strain controlled fatigue testing is preferred to load controlled for this research, because it enables study of low cycle fatigue resulting from plastic behaviour of the material at load levels above the yield strength. Whereas load controlled fatigue testing is only applicable to load levels below the yield strength where the material responds elastically.

Work performed over the last two years are reported in two sections: (1) high cycle fatigue (HCF), (2) fatigue crack growth rate properties. These properties are related to the safe-life and damage tolerance design of AM metallic components. Key findings are summaries at the end of each section. For more information about the research programme, the latest publications and findings visit the website https://newam.uk/

Three different deposition strategies were used, namely single pass, parallel pass, and oscillation wave builds as shown in Fig. 1. The single pass build is limited to a maximum thickness of around 8 mm, whereas the other two methods can build thicker materials as well as parts with variable thickness. All samples were tested in the as-built condition with standard surface machining and polishing. Test samples for the HCF and crack growth rate properties are distinguished as either “horizontal (H)” or “vertical (V)” with respect to the material build direction. In the parallel pass build, four parallel passes in each layer are aligned in the WD direction; the four tracks were deposited consecutively with a 50% overlap between the passes. For each track, the process head was translated along the wall length direction. In the oscillation build, the plasma torch and the wire feeder were continuously oscillated across the wall thickness direction (TD) with about 50% overlap between the melt tracks as the process head progressively translating along the wall length direction (WD).

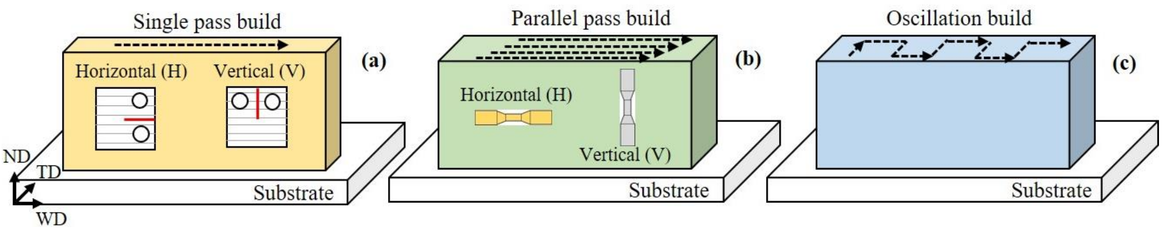

Fig. 1: Schematic of WAAM Ti64 walls (a) single pass, (b) parallel pass, (c) oscillation deposition strategies. WD: welding heat source travel direction, TD: transverse direction, ND: normal direction. Extracted test samples for fatigue crack growth and HCF are also shown.

3.2.2 Strain-controlled fatigue tests

This work presents material behaviour and properties in fully reversed low cycle fatigue (LCF) and high cycle fatigue (HCF) regimes for WAAM Ti-6Al-4V in as-deposited condition. X-ray computed tomography was used to detect defects in the test samples. A detailed microstructure and fractography was performed to understand the role of microstructure on crack initiation and fracture. The following key findings are discussed with respect to the characteristics of the microstructure:

- Cyclic stress-strain curves obtained from fatigue hysteresis loops show typical cyclic softening. Horizontal build orientation samples, with the loading axis perpendicular to the columnar β grains, showed higher material performance. This finding aligns with static tensile test data where horizontal samples showed higher yield and tensile strengths.

- In the LCF region (<10^4 cycles), vertical build orientation samples, loaded along the columnar β grains, is superior. This is considered to be linked to the microstructure along the grain boundary α.

- In the HCF region (>10^4 cycles), vertical and horizontal build orientation sample performance is similar, though with considerable scatter in the data.

3.2.2 Stress controlled fatigue (HCF)

HCF properties were investigated only for the oscillation and parallel pass builds. Fig. 2 shows the test results in two sample orientations. Fatigue data for the mill annealed wrought sheet (2 mm thick, L-T orientation) and a cast plate (12.7 mm thick) are also presented. Fatigue strength of the WAAM specimens was higher than the cast material and only marginally lower than the wrought, except the oscillation build horizontal samples tested at 500 MPa. Of the two deposition strategies, the parallel pass build showed a marginally higher fatigue life than the oscillation build.

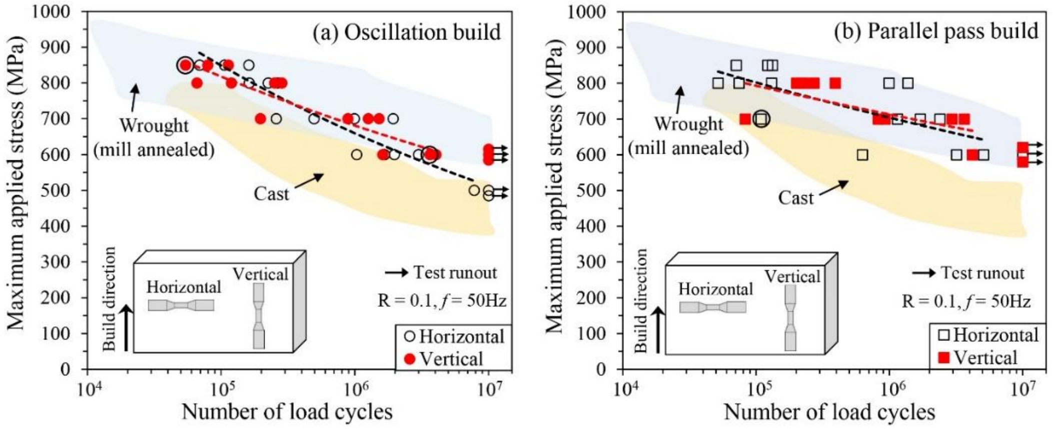

Fig. 2: S-N data for the oscillation and parallel pass builds and best fitted lines. Encircled data points indicate crack initiation from a surface pore. Their wrought [2] and cast [2] counterparts are also shown.

Since the parallel pass build had much finer α laths (0.93 µm) than that of the oscillation build (2.27 µm), the marginally higher fatigue strength in the parallel pass build is due to the lower cyclic slip length. Figure 3 also shows a mild anisotropic behaviour in the oscillation build, where at 10^7 cycles, the vertical samples had higher fatigue limit (600 MPa) than the horizontal samples (500 MPa). There is virtually no difference in the fatigue limit in the parallel build between the two crack orientations. Also, fatigue strengths of the horizontal samples in both builds are similar when the applied maximum stress is greater than 700 MPa. Based on the β grain width, we can say that the oscillation build had fewer β grains per unit volume compared to the parallel pass build. The majority of α_{GB} in the oscillation build consists large α colonies oriented in one direction indicating a strong crystallographic texture along the α_{GB}. In contrast, the parallel pass build showed fine α colonies that are randomly oriented with weaker texture. In horizontal samples, the α_{GB} is perpendicular to the fatigue loading, where the majority of the single variant large α colonies are under fatigue loading and greatly influence the crack initiation, thereby fatigue life [3]. Hence fatigue property anisotropy is found. On the other hand, the weaker texture along the α_{GB} in parallel pass horizontal samples might not have influenced the fatigue life. Therefore, fatigue property anisotropy was not found.

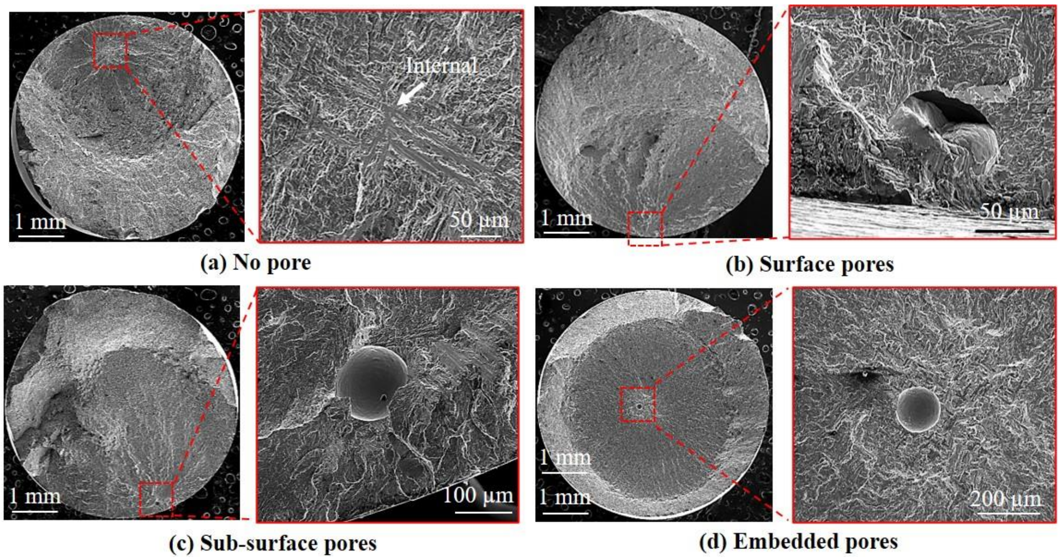

Fig. 3: SEM images of fracture surfaces (left) and crack initiation location of the corresponding sample in higher magnification (right).

Fracture surface analysis showed two different sources for crack initiation. Based on the crack initiation source and location, the SEM images are presented in four groups in Fig. 3; a) no defect, where crack initiated from a microstructure feature on the sample surface or internal (20% of the test data), b) crack initiation from a surface pore (4%), c) crack initiation from a subsurface pore with distance to the surface being less than four times of pore diameter (18%), d) crack initiation from an internal defect (47%). The rest minority was test runouts (i.e. sample did not fail at 10^7 cycles). All the pores had spherical morphology and were predominantly attributed to entrapped gas. Pore sizes were considered as very small, with diameters of 20-110 µm in the oscillation build, and 5-140 µm in the parallel pass build.

Based on our previous study [4], we have considered 100 µm pore diameter as a threshold value for WAAM Ti64. Majority of the crack initiating pore sizes was below the threshold value 100 µm. Such small pores may be the consequence of the wire quality, and may be realistic for the feedstock we commonly get, hence the S-N data presented in Fig. 2 can be regarded as the material intrinsic property (i.e. the same as those without any pores). In addition to the porosity size, the surrounding microstructure and crystallographic texture at the pore might have also contributed to the scatter in the test data.

Details of the work reported this section can be found in a recent paper [5].

<u>Key findings</u>:

- Fatigue strength at 10^7 cycles was 500 MPa for the oscillation build horizontal samples and 600 MPa for all other cases (i.e. oscillation build vertical and both orientations in the parallel pass build). The finer transformation microstructure in the parallel pass build resulted in greater resistance to crack initiation, thereby higher fatigue limit than the oscillation build when comparing the horizontal samples.

- Small gas pores were the primary source of fatigue crack initiation and caused large scatter in the test data. Fractography revealed an average pore size of 70-75 µm in both build strategies. About 70% of samples had crack initiation from small pores, and 20% samples had crack initiation from a microstructure feature (i.e. no pores were found).

3.2.3 Fatigue crack growth rates

Fatigue crack growth rates were investigated for three build strategies: single pass, parallel pass, and oscillation build, and in both horizontal and vertical crack orientations. Measured crack growth rates are presented in Fig. 4, along with trend lines for the equivalent Ti64 alloys produced by traditional methods of forging and casting.

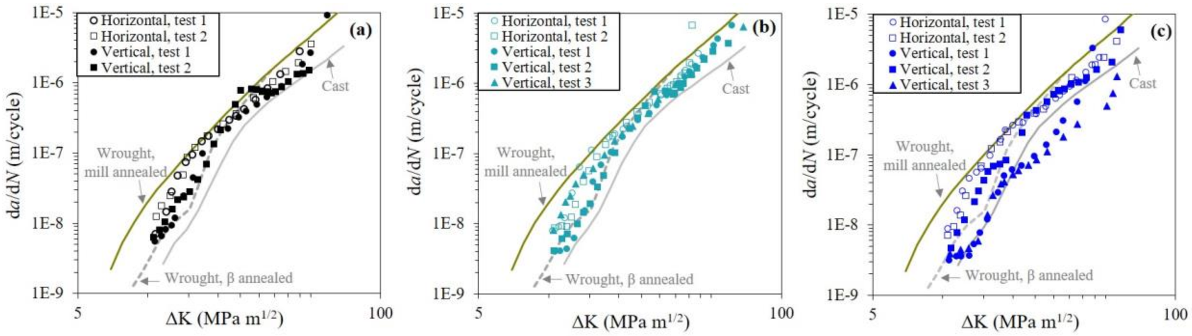

Fig. 4: Fatigue crack growth rate: (a) single pass, (b) parallel pass, (c) oscillation builds, and comparison with conventional Ti64 alloys from AMS 4992: β annealed cast (10 mm thick)[2], β annealed wrought (L-T, 10 mm thick, 1050°C 1hr, furnace cooling, stabilisation annealing 730°C 2hr, furnace cooling)[6], and mill annealed wrought plates (L-T orientation, 6.35 mm thick)[2].

When Δ*K* is below 12 MPa√m, the crack growth rates for single pass and parallel pass build fall below the value of the typical mill annealed wrought material but are above the value of a cast or wrought β annealed material. This ranking of crack growth rates is expected, given that coarse lamellar single α variant colony microstructures are expected to cause higher levels of crack deflection and crack closure, which reduce the effective Δ*K*, hence the crack growth rate. It is therefore expected that a finer multi-variant basketweave microstructure might fall somewhere between these two extremes. Despite the scatter in the test data, a trend can be seen that the crack growth rate is higher for the horizontal samples (crack across the columnar grains) by a factor of around two at lower Δ*K* (< 20 MPa√m), especially in the single pass build.

Compared to the single pass and parallel pass builds, the oscillation build showed much more scatter in test data, greater property anisotropy, and significantly lower crack growth rate in the vertical samples, by one magnitude. Among the three vertical crack samples in the oscillation build, tests 1 and 3 showed lower crack growth rates by a factor of around three for Δ*K* values below 25 MPa√m. The reasons for the greater property anisotropy at lower Δ*K* can be related to the microstructure influence, as the microstructures are different among the builds. All the samples showed local crack deflection at quite short crack length (0.5 mm from the notch tip). However, greater influence of the α colonies on crack deflection was observed in the oscillation build that had the lowest crack growth rate. This difference in behaviour can be mainly attributed to the presence of larger and more defined multi-variant (basketweave) α colonies within the β grains. In addition, a wider layer of single variant α colonies is present on the β grain boundaries. Stronger microtexture variation in the oscillation build also caused more substantial crack path deflection in the vertical samples, which can alter the mode-I fracture to a mixed mode I and II, which reduces the mode-I crack growth driving force, thereby reduce the crack growth rate [7].

To further elucidate the lower crack growth rate and greater crack path deflection seen in the oscillation build vertical samples, electron backscattered diffraction (EBSD) inverse pole figure maps (coloured with respect to ND) were performed for the vertical samples produced by all three build methods. The higher cooling rates in the single pass and parallel pass samples had limited deflection as they cross the colony boundaries. In contrast, in the oscillation build sample, both macroscopic crack path and greater local crack deflection can be observed. After the crack initiation just above the primary β grain near the machined notch, the crack is deflected downwards and followed a path influenced by the microstructure of multi-variant (basketweave) α colony within the coarse β grain, which makes up the majority of the grains in the oscillation builds. This contributed greatly to scatter in the crack growth rate, particularly in the near threshold regime. The lower scatter seen in the single and parallel pass builds was caused by the considerable finer basketweave α transformation structure due to the lower local heat input in these two processes. This would be expected to lead to less crack deflection within a β grain and a flatter crack surface.

Details of the work reported this section can be found in a recent paper [8].

<u>Key findings:</u>

Comparing to traditional processed Ti64, fatigue crack growth rate in WAAM Ti64 is lower than the mill annealed wrought, but higher than the beta annealed wrought and casting materials.

The parallel path deposition method showed higher crack growth rate than the oscillation build when the crack is growing across the layers. However, there was virtually no difference between the two build methods when the crack is propagating parallel to the layers.

Anisotropic behaviour between the two major crack orientations was observed only for the oscillation build.

References

[1] Kobryn P, Semiatin S. Microstructure and texture evolution during solidification processing of Ti–6Al–4V. J Mater Process Technol 2003;135:330–9. doi:10.1016/S0924-0136(02)00865-8.

[2] Metallic Materials Properties Development and Standardization (MMPDS-04). 2008.

[3] Shamir M, Syed AK, Janik V, Biswal R, Zhang X. The role of microstructure and local crystallographic orientation near porosity defects on the high cycle fatigue life of an additive manufactured Ti-6Al-4V. Mater Charact 2020;169:110576.

doi:https://doi.org/10.1016/j.matchar.2020.110576.

[4] Biswal R, Zhang X, Syed AK, Awd M, Ding J, Walther F, et al. Criticality of porosity defects on the fatigue performance of wire + arc additive manufactured titanium alloy. Int J Fatigue 2019;122:208–17. doi:10.1016/J.ijfatigue.2019.01.017.

[5] Syed AK, Zhang X, Caballero A, Shamir M, Williams S. Influence of deposition strategies on tensile and fatigue properties in a wire + arc additive manufactured Ti-6Al-4V. Int J Fatigue 2021; 149:106268. doi:https://doi.org/10.1016/j.ijfatigue.2021.106268.

[6] Seo W, Jeong D, Lee D, Sung H, Kwon Y, Kim S. Effects of cooling rate and stabilization annealing on fatigue behavior of β-processed Ti-6Al-4V alloys. Met Mater Int 2017;23:648–59. doi:10.1007/s12540-017-6730-9.

[7] Leitner T, Hohenwarter A, Ochensberger W, Pippan R. Fatigue crack growth anisotropy in ultrafine-grained iron. Acta Mater 2017;126:154–65. doi:10.1016/J.ACTAMAT.2016.12.059.

[8] Syed AK, Zhang X, Davis AE, Kennedy JR, Martina F, Ding J, et al. Effect of deposition strategies on fatigue crack growth behaviour of wire + arc additive manufactured titanium alloy Ti–6Al–4V. Mater Sci Eng A 2021;814:141194. doi:https://doi.org/10.1016/j.msea.2021.141194.

4 Enhancing fatigue performance

4.1 Laser peening fatigue research – Cranfield University

D.O. Busse, S. Ganguly, D. Furfari, P.E. Irving – Cranfield University

Cranfield University continues to perform fatigue research supporting design and manufacture of aluminium aircraft structures. Current research builds on previous work in collaboration with Airbus on fatigue life prediction of friction stir welded aluminium sheet and plate, and the improvements laser peening can bring to fatigue strength of mechanically fastened joints. Laser peening is an effective way to induce a surface compressive residual stress state in aerospace aluminium alloys, which helps prevent initiation and reduces propagation of fatigue damage.

4.1.1 Laser peening of bolted lap joints

Recent research has explored via experiments and modelling the improvements in fatigue life given by laser peening of 2024 aluminium bolted overlap joints.

Fatigue tests were performed on 3-row 15 hole overlap joints in which the outer hole rows (containing 5 holes) were laser peened on the contacting faying surfaces prior to joint assembly. The effect of four different peening patterns shown in figure 1 were investigated. These were:

1. A continuous peened strip covering all 5 holes in the outer rows.
2. Individual peen patches surrounding each hole in the row with gaps between them.
3. A continuous strip as in (1) but with the strip width significantly extended in the loading direction so as to terminate outside the joint assembly.
4. With patches as in (2) but with the patch widths extended to terminate outside the joint assembly.

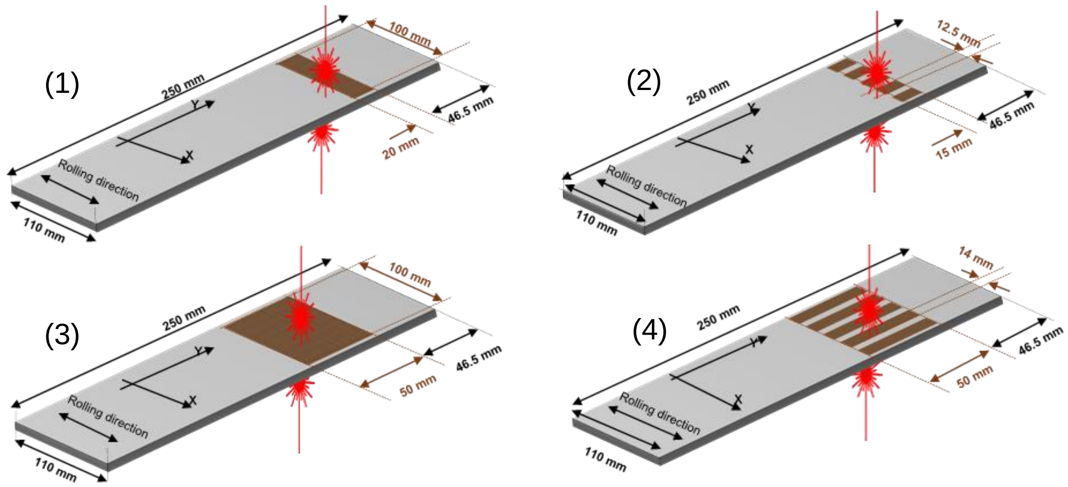

Figure 1: Peening patterns applied to bolted lap joint elements prior to assembly.

After peening residual stresses were measured using hole drilling and synchrotron source X ray diffraction, followed by joint assembly. Tension – tension fatigue testing was performed with an R ratio of 0.1 on all peened samples and for comparison, unpeened samples of identical geometry were also tested. In unpenned samples fatigue cracks always initiated in fretting adjacent to the outer hole rows under conditions of maximum bend stress. Peening always improved the mean fatigue life, as shown in figure 2, but the extent of improvement depended on the peen pattern treatment. In peened samples in addition to fretting initiation at the same location as in unpeened samples, fatigue cracks initiated at locations remote from the holes, outside the boundary of the peened area. While the peened areas contained significant compressive residual stresses, outside the peened area there were balancing residual tensile stresses. Samples with marginal improvements in fatigue life, had initiation exclusively from regions of tensile residual stress. The best fatigue life was found in peening pattern 4, which more than tripled the life. In pattern 4 samples cracks initiated both in fretting under compression stress and in normal fatigue at locations subjected to tensile residual stress, suggesting that both modes have similar fatigue lives in this case.

The research demonstrates that introduction of local compressive residual stresses into surface regions improves local fretting fatigue life, but creation of balancing tensile residual stresses will reduce fatigue life at alternative initiation sites. The reduction may be sufficient to cause fatigue initiation at this location to be preferred, thus limiting the net life improvement provided by the compressive stress. Optimum fatigue life requires a balance between compression stresses improving fretting fatigue life, and balancing tensile stresses reducing fatigue life elsewhere.

A paper on this work will be submitted shortly to International Journal of Fatigue.

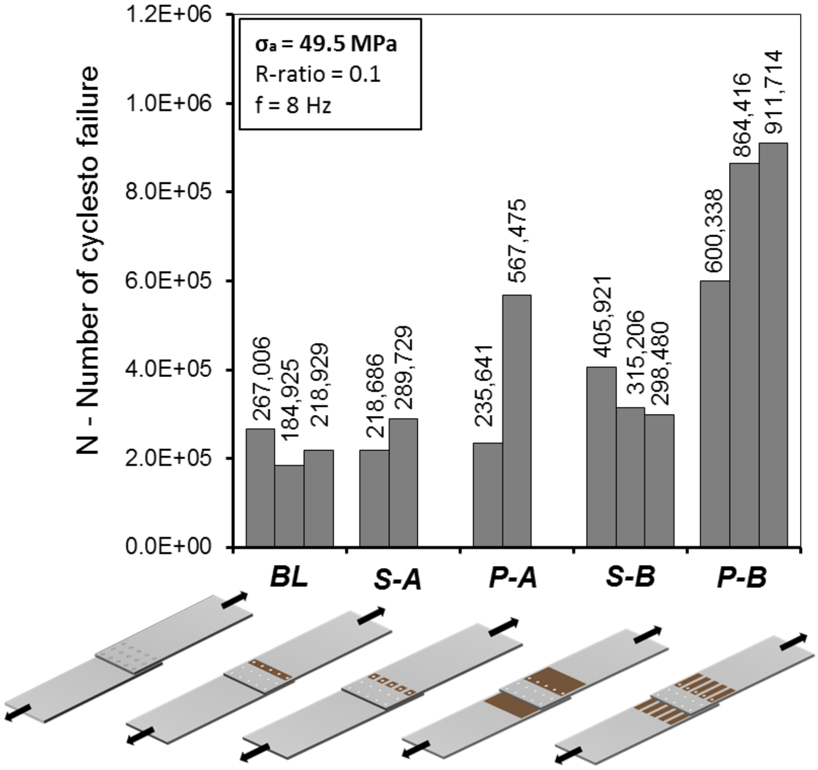

Figure 2: Histogram of the fatigue lives of peened and unpeened joints. The peening pattern corresponding to each group of histogram bars are shown below the chart.

4.1.2 Laser peen crack retarders

In experimental work on fatigue crack growth in 400 mm wide centre cracked panels (CCT) of 1.6 mm thick 2024 aluminium it was demonstrated that 30 mm wide laser peen strips introduced into the path of propagating fatigue cracks could successfully reduce the local fatigue crack growth rates by up to a factor of 10 and promote an increase in overall crack growth life. Residual stress measurements showed the peened areas contained compressive residual stresses of 100 MPa In addition to the retardation observed within the peened area, crack growth acceleration was found under the influence of the balancing tensile stresses encountered by the crack tip before it entered the peened area. Overall crack growth life was therefore a balance between retardation and acceleration as the crack progressed across the residual stress field.

To investigate factors controlling crack growth rates, a 2D finite element model of the CCT panel containing regions of compressive and balancing tensile residual stress was constructed. Compressive residual stress within the peen patch, distance of the patch from the CCT centre notch, peen patch width, level of external cyclic stress were all systematically varied. The effect of having additional identical peen patches in the crack path was also explored. A crack growth rate simulation model was constructed using a modified superposition approach in which the combined effect of external cyclic stress and internal residual stresses on ΔK_{eff} the effective stress intensity was calculated and was used in turn to derive local crack growth rates and crack length vs. cycles curves.

The simulations predicted a wide range of fatigue crack growth rates and lives depending on the initial local conditions. Many combinations of factors were detrimental, producing reduced fatigue lives rather than increased ones. The position and extent of the peened region significantly influenced balancing tensile stress field and hence fatigue life, even though the residual compression field was constant. Whether overall life is greater or less than the unpeened samples depends on the balance between retardation and acceleration stages. Inserting more than one peened region into the crack path had marginal effects on overall life, while the external loading had a more profound effect; largest retardations being found at small external loads, with little or no effect at large values of ΔK near to final failure. These factors all require incorporation into design of a practical crack retardation system to improve damage tolerance. A summary of the important aspects of the work is published at *Busse D, Ganguly S, Furfari D, Irving PE 2020 “Optimised laser peening strategies for damage tolerance aircraft structures” Int J Fatigue 141 -105890.*

4.1.3 Laser peening of friction stir welded aluminium alloys

This work in progress is exploring the benefits which laser peening can provide to fatigue performance of friction stir welded aluminium sheet. Particular attention is being given to the role of Lack of Penetration defects (LoP) in determination of fatigue life and the extent to which Laser Peening can eliminate defect sensitivity.

Since the start of this project, activities carried out include: hole drilling measurements to quantify the bi-axial residual stress in peened samples treated with different laser process parameters; fatigue tests to determine the life of unpeened welded components; fracture analysis of fatigue specimens to identify crack initiation locations and correlate them with defect and residual stress distribution through the cross section. A finite element model has been developed to calculate stress intensity factors at the tip of a crack-like LoP defect under the combined influence of residual and externally applied stresses and so investigate threshold conditions for crack growth and optimisation of the fatigue life.

Fatigue testing on unpeened welded samples has shown that 400 µm depth LoP defect in the weld acts as a crack initiation site, decreasing fatigue life by approximately 90% compared to the as-welded condition, and inducing failure from the weld root. Smaller defects 200 µm deep have less of an effect, producing lives similar to friction stir welds without defects but retaining the as welded surface relief.

Future work will fatigue test peened samples produced according to the results from the parameter optimisation study, in order to be able to quantify the increase in life from specimens having the same characteristic defects.

4.2 Crack trajectory modifications and life extension due to laser peening residual stress

M. Leering, M. E. Fitzpatrick, N. Smyth, X. Zhang - Coventry University

In the period from 2019 – 2021, the Structural Integrity Research group at Coventry University has continued to study the uses of Laser Shock Peening (LSP) as a life enhancement technique for aerospace structures. The work has been sponsored by Airbus and the United States Air Force Research Laboratory, with laser peening support from the Council for Scientific Research – National Laser Centre, South Africa, and Hilase, Czech Republic.

We have investigated the potential use of laser peening residual stresses as a tool to achieve crack trajectory modifications and extension in service life. This was achieved by introducing LSP patches that draw the cracks towards the area of the high compressive residual stress and reduces the driving force of the crack. Two angled laser peened patches are placed on either side of a centrally propagating crack which was exposed to a mode I tension-tension loading configuration. It was found that the cracks propagated roughly perpendicular to the loading direction until nearing the LSP induced residual stress field, as shown in Figure 1. The combination of the applied loading and the LSP residual stress created the necessary biaxial stress state at the crack tip to initiate mixed-mode loading which caused the deviation of the crack trajectory.

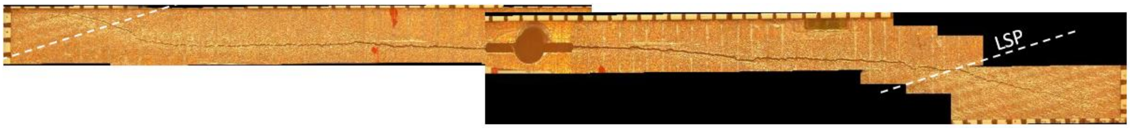

Figure 1: Fatigue crack trajectory modifications by laser shock peening induced residual stress fields

An additional benefit of the presence of the LSP residual stress was the life improvement that occurs due to the reduction in crack growth rate. Figure 2 shows the effects of the angled LSP patches on the crack growth rate of the peened component indicating the service life was improved by as much as 7.5 times the original life. The extent of the life improvement was dependent on the angle and relative positioning of the LSP patches to the initial crack notch.

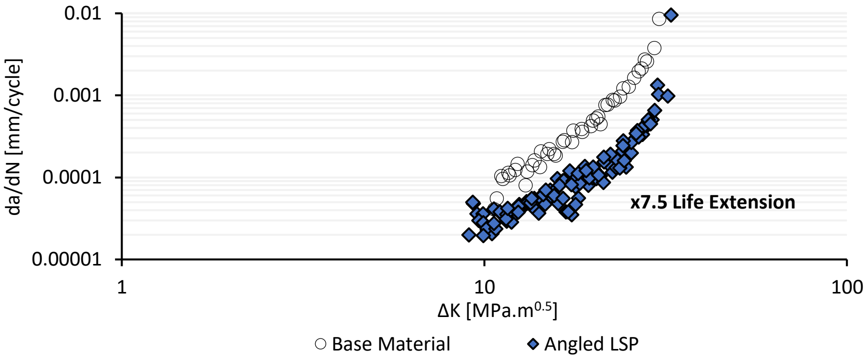

Figure 2: Effect of angled laser peened patch on fatigue crack growth rate

Figure 3 shows the finite element modelling of the crack growth process that was conducted to study the effects of the residual stress on the mode I and II crack growth rates as the crack was propagated across the angled LSP sample. The figures show that the presence of the LSP residual stress created an additional $K_{II,res}$ component which was large enough to establish a modification in the trajectory of the crack: with the highest expected deviation occurring just outside the LSP patch, due to the LSP balancing tensile residual stresses which occur adjacent to the patches. The finite element results were used to provide a fairly accurate prediction of the expected fatigue crack growth rate in the presence of LSP residual stresses.

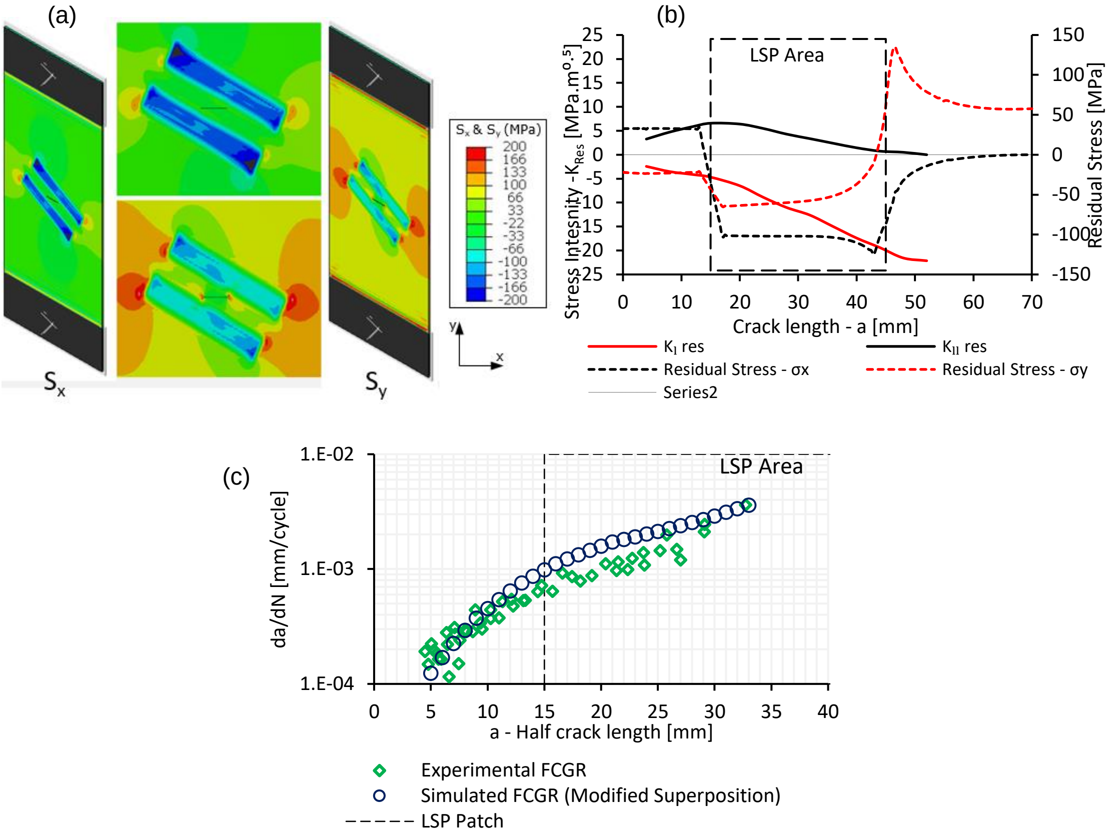

Figure 3: (a) finite element analysis of a crack in the presence of a laser peening induced residual stress field, (b) residual stress established $K_{I,res}$ and $K_{II,res}$ across the crack path of the angled laser peening samples, (c) comparison of the experimental and predicted fatigue crack growth rates

It was concluded amongst other insights that:

- The deviation in the fatigue cracks was primarily caused by the balancing tensile stresses that occur in the external regions of the LSP patch, with the crack pulled toward the LSP patch.
- The largest modification in the trajectory occurred by placing the LSP patches further along the crack path whilst the largest extension in life is achieved by placing the patches nearer to the notch.

Recent relevant papers:

- A.G. Sanchez, C. You, M. Leering, D. Glaser, D. Furfari, M.E. Fitzpatrick, J. Wharton, P.A.S. Reed, ‘ Effects of laser shock peening on the mechanisms of fatigue short crack initiation and propagation AA7075-T651’. Intl J. Fatigue. 2021:143:106025. DOI: 10.1016/j.ijfatigue.2020.106025

- Angulo, F. Cordovilla, A.García-Beltrán, N.S. Smyth, K. Langer, M.E. Fitzpatrick, J.L. Ocaña, ’The effect of material cyclic deformation properties on residual stress generation by laser shock processing’. Intl J. Mech. Sci. 2019:156:370-381 DOI: 10.1016/j.ijmecsci.2019.03.029

- M. Pavan, M. E. Fitzpatrick, D. Furfari, B. Ahmed, M. Gharghouri, ‘Fatigue Crack Growth in a Laser Shock Peened Residual Stress Field’. Intl J. Fatigue. 2019:123:157-167. DOI: 10.1016/j.ijfatigue.2019.01.020

- N. Smyth, M. B. Toparli, M. E. Fitzpatrick, P. E. Irving, ‘Recovery of fatigue life using laser peening on 2024-T351 aluminium sheet containing scratch damage: the role of residual stress’. Fatigue Fracture Engng Mater. Struct. 2019:42:1161-1174. DOI: 10.1111/ffe.12981

- M. B. Toparli, M. E. Fitzpatrick, ‘Effect of overlapping of peen spots on residual stresses in laser peened aluminium sheets’. Metall. Mater. Trans. 2019:50(3):1109-12. DOI: 10.1007/s11661-018-05100-0

5 Understanding fatigue behaviour

5.1 Microstructure-sensitive prognosis of fatigue crack nucleation

G.M. Castelluccio - Cranfield University

Fatigue crack nucleation is strongly controlled by microstructural attributes such as grain size, morphology, and crystallographic orientation. Crystal plasticity models have been successful in predicting the role of microstructure and life variability. However, these models rely on multiple parameters that are not usually unique: multiple sets of parameters result in equivalent responses. The origin of this lack of uniqueness relies on the limitations of the experimental data available for identifying the parameters.

This research has focused on developing monotonic and cyclic crystal plasticity models that can match single- and polycrystals for various materials. Our work has demonstrated that fitting to polycrystals is not enough reproduce the local mechanical response at the grain level. As a result, the lack of local validation (grain level) can obscure the real variability.

We have applied these models to investigate crack nucleation in small statistical volumes undergoing cyclic loading. We recreated multiple microstructural computational realizations to estimate fatigue crack nucleation lives and orientations by means of physics-based approaches. Our work demonstrated a unique approach to validate microstructure sensitive models and quantify the fatigue crack stochasticity associated with small volumes.

In addition, we have also innovated with reduced order models that predict crack nucleation variability from notches without need to run computationally demanding crystal plasticity models for each new geometry. As a result, statistical assessments for fatigue crack nucleation can be informed with low-cost computational models.

https://www.sciencedirect.com/science/article/pii/S014211232030164X
Ashraf, Castelluccio. Proceedings of Fatigue 2021.

5.2 Integrated approaches to understand the transition from corrosion to mechanical driven cracks at high temperature

S. Gray, G.M. Castelluccio - Cranfield University

Turbine engines' air intake can result in the deposition of corrosive species on single-crystals blades and lead to early crack nucleation and accelerated degradation. Crack initiation typical occurs along cube plane in crystals and can extend for hundreds of microns. Upon further cyclic loading, cracks change into octahedral plane, typical of mechanical loading. The mechanisms responsible for the damage and the change in morphology depend on the temperature of operation and stress level, but they are yet not fully understood.

This research has focused on understanding the role of different salts on the scale formation and crack initiation of CMSX-4 at 550 °C. On the one hand, we perform extensive experimental analysis exposing single-crystal Ni-base superalloy C-rings to salts at high temperatures for different periods. The findings suggest that the sulphation of chlorine-containing species in sea salt led to the formation, vaporisation, and re-oxidation of metal chlorides, and this mechanism was found to play a key role in the formation of a non-protective scale. In parallel, we are developing computational models capable of reproducing the cube to octahedral cracking transition with the goal of understanding which loading conditions promote either damage mechanism.

https://link.springer.com/chapter/10.1007/978-3-030-51834-9_73

6 Non-destructive testing

6.1 Development of a protocol for model-assisted qualification (MAQ) of NDT techniques

D. Hallam – Defence Science and Technology Laboratory (Dstl)

Despite Non-Destructive Testing (NDT) being one of the primary tools required to support the continuing airworthiness of aircraft structures and systems, there remains considerable difficulties introducing new NDT capabilities into service. A proposal to address the main issues, by developing a Model Assisted Probability of Detection (MAPOD) approach, was proposed by Professor Robert Smith, Professor of NDT and High-Value Manufacturing at the University of Bristol and reported in the Military Aircraft Structural Airworthiness Advisory Group (MASAAG) Paper 122.
A Dstl-sponsored programme of work led by TWI and supported by ESR Technology, University of Bristol and BAM commenced to create, draft and demonstrate a protocol for model-assisted NDT technique validation for military air-domain applications. The primary focus was delivery of a generic protocol that reduces the cost of Probability of Detection (PoD) studies through use of a smaller number of samples combined with physics-based models. The protocol consists of three main parts; a flowchart, a step-by-step guide describing the steps to consider in order to implement a model assisted qualification approach for NDT inspections, and an appendix of supporting information. Figure 1 shows the final condensed version of the protocol flowchart.
The protocol approach has primarily been demonstrated for ultrasonic inspection for metallic aerospace materials with its suitability tested by performing a number of experimental trials. Guidance on how to minimise the effects of human factors, along with paper case studies to account for automated acquisition, analysis and sentencing; large area inspection and SHM; and the composite materials have been included in the protocol as appendices. Efforts are now underway to publish this protocol to encourage wider adoption.

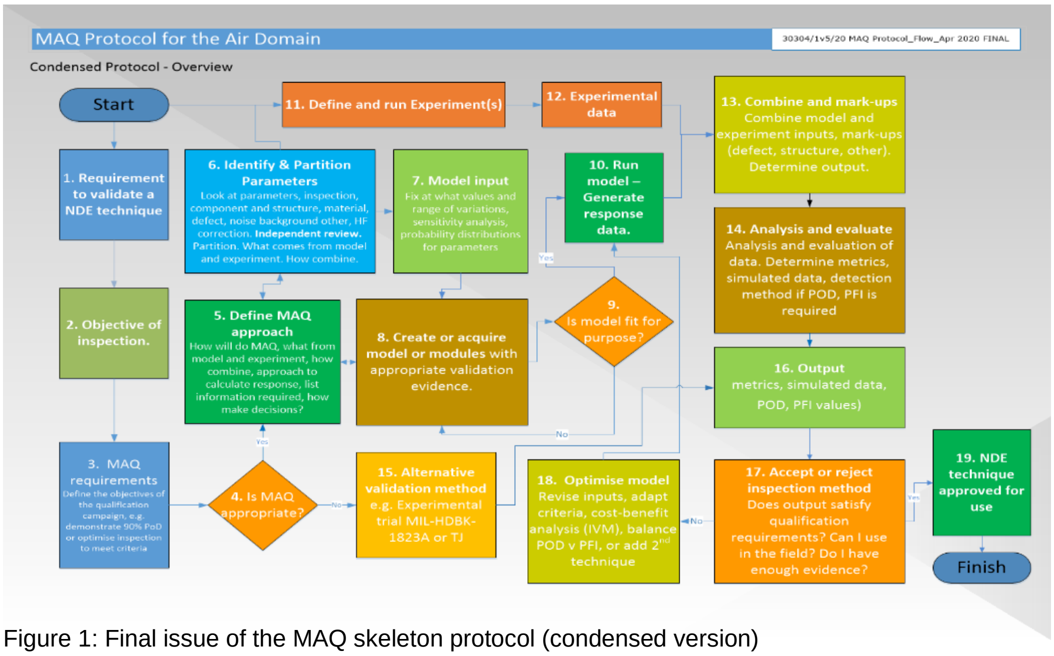

Figure 1: Final issue of the MAQ skeleton protocol (condensed version)

7 Structural health monitoring

7.1 Development of a Wireless Acoustic Emission Monitoring System for Aerospace

S. Grigg, C. Featherston & R. Pullin - Cardiff University*
*pullinr@cardiff.ac.uk

7.1.1 Introduction

Impact and fatigue have the potential to cause the initiation and growth of damage during an aircraft structures' life. The detection of this damage when it grows is beneficial, as it enables repairs to be conducted when required, rather than during scheduled maintenance, this process is known as structural health monitoring (SHM). SHM could lead to improved safety, reduced maintenance costs and even lighter aircraft if SHM systems can be relied upon and redundancy reduced. There is a drive for these systems to be wireless, which significantly reduces weight and saves on instillation costs.

When damage occurs, energy is released in the form of ultrasonic stress waves, known as Acoustic Emission (AE). These waves propagate within the boundaries of the structure and can be detected using piezoelectric sensors. Using an array of sensors over the structure allows for localisation for these events which indicates the potential presence of damage. However, this approach is not feasible for a low power wireless system as accurate time synchronisation is very power intensive, and the available power on an aircraft through energy harvesting in minimal.

In plate like structures AE travels as Lamb waves, primarily in the S_0 and A_0 modes. These modes differ in their frequency, the S_0 consisting of primarily higher (>200 kHz) and the A_0 lower (<100 kHz). They are also known to travel at significantly different velocities (the S_0 being faster), meaning that if their arrival times are known, the difference in these makes it possible to predict the distance the wave has travelled. Three closely spaced sensors have also been shown to enable trigonometric approaches based on the arrival of a waveform, to find the angle of arrival. The combination of these two techniques allows the location of a source to be found. The advantage of this approach in for a wireless system is that there is no need to high accuracy time synchronisation between nodes. This work gives a brief overview of the development of a low power wireless AE system that applies this approach, and some initial testing results.

7.1.2 Hardware Overview

The use of three closely spaced sensors to locate AE sources in plate like structures is well documented, previously this was done using continuous wavelet transform (CWT), which show the frequency of the signal relative to time. To determine a modes arrival the point at which its dominant frequency crosses a threshold in the CWT is found. Although this approach is effective, it's computationally demanding, which is infeasible in a low power system. Instead, for this sensor node front end analogue filters were used, the A_0 mode isolated using a 60 - 140 kHz band pass filter and the S_0 mode using a 140 – 300 kHz band pass filter. The mode was deemed to have arrived when it crossed a threshold on each channel. Once arrival times were determined the node predicts the angle of arrival and distance to the source; parameters are also extracted from an unfiltered waveform. This data is then and transmitted wirelessly to a central hub via RF. The node is shown in Figure 1 alongside sensors bonded to a complex composite panel.

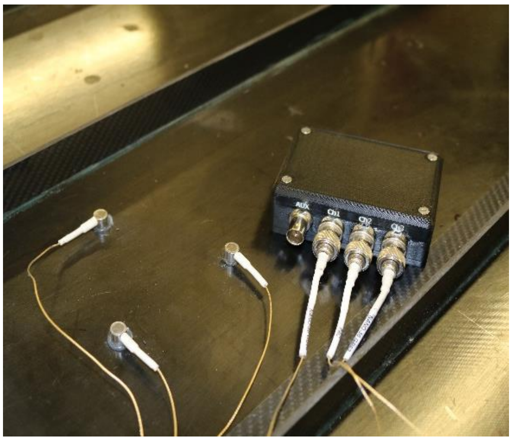

Figure 1: Wireless sensor and PZT's on composite panel

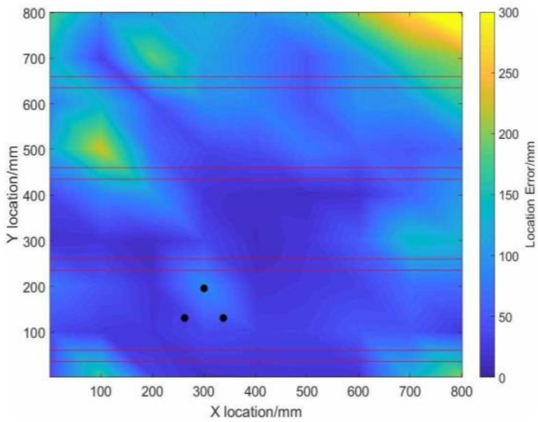

Figure 2: Absolute location error of sensor node on complex composite panel. Sensors in black, stiffeners in red.

7.1.3 Testing

The hardware was initially tested in a variety of use conditions and the power consumption analysed. The results for this testing is shown in Table 1.

Location accuracy testing was then conducted on a 0.9 m x 0.9 m quasi-isotropic composite plate with a layup of $(0/45/90/-45)_{2S}$. Four stiffeners were then attached to each plate, all with Araldite A/B. Three Mistras Nano-30 sensors were bonded in a 75 mm triangle, these were off centre from the middle of the panel as initial testing showed the range on the node to be greater than possible to test if bonded in the centre. Hsu-Neilson sources (mechanical pencil lead brake - the ASTM standard for sensor calibration) were then conducted at 50 mm spacing over the panel to test accuracy.

The absolute location error for the composite panel testing is shown in Figure 22. Here the average absolute error is 101 mm. This is produced by an average angle error of 4.7º and average angle distance prediction error of 68.7 mm.

Table 1: Power consumption of node in a variety of functions/performing certain tasks

	Sleep	Event Monitoring	RF Listen Window	Event processing	RF Transmission
Time (ms)	-	-	103	5	176
Average Power (mW)	0.33	17.44	43.4	10.0	39.5
Total Energy (mJ)	-	-	4.47	0.05	6.95

7.1.4 Further Reading

For further information on this sensor node and the results of testing on a wide range of structures, please refer to “*Development of a Low Power Wireless Acoustic Emission Sensor Node for Aerospace Application*” by Grigg et al. published in Structural Control and Health Monitoring 2021.

7.2 Structural Health Monitoring, Manufacturing and Repair Technologies for Life Management Of Composite Fuselage - SHERLOC

F. Aliabadi - Imperial College London

Duration: 7 years
Overall Budget ≈€10m: Starting Date: 01/09/2015 **End Date:** 01/09/2022
Coordinator: Prof. Dr. Ferri M H Aliabadi, Zaharoff Chair in Aviation, Imperial College London, UK

Design and maintenance of future pressurized fuselage composite structures is mainly influenced by the requirement to cope with accidental impact damages. SHERLOC's central aim is the development of a Condition Based Maintenance (CBM) concept for composite fuselage enabled by Structure Health Monitoring (SHM) techniques. The industrial uptake of Structural Health Monitoring is aimed at markedly improving safety and reducing maintenance that are currently estimated to be around quarter of the aircraft fleet's operating cost. SHERLOC's main focus is: sensor technology, system validation and integration, global systems and regulatory guidance. The key components of the SHERLOC SHM prototype system are: Diagnosis, Prognosis and Life Extension and Predictive Maintenance. SHERLOC has developed a SHM system based on Piezoelectric (wired and wireless), Fibre Optics, Hybrid and Magnetostrictive technologies for damage detection and repair. The system has been verified and validated through the building block approach at three levels of coupon, element (skin/stringer, aft, window frames, floor structures) and subcomponent (real scale flat and curved composite panels), see figure 1. The operational conditions have been taken into account to demonstrate the SHM technology operating in industrially relevant conditions (TRL6). SHERLOC has paid particular attention to SHM system installation and manufacturing (automatic placement of pre-preg technique, RMT and thermoplastic forming). SHERLOC's novel Bayesian based Dynamic Data Driven Application System (DDDAS) that will allow the characterization of uncertainty and conditional probabilities to be determined in terms of what is known about the structure from the model and what is measured during the inspection.

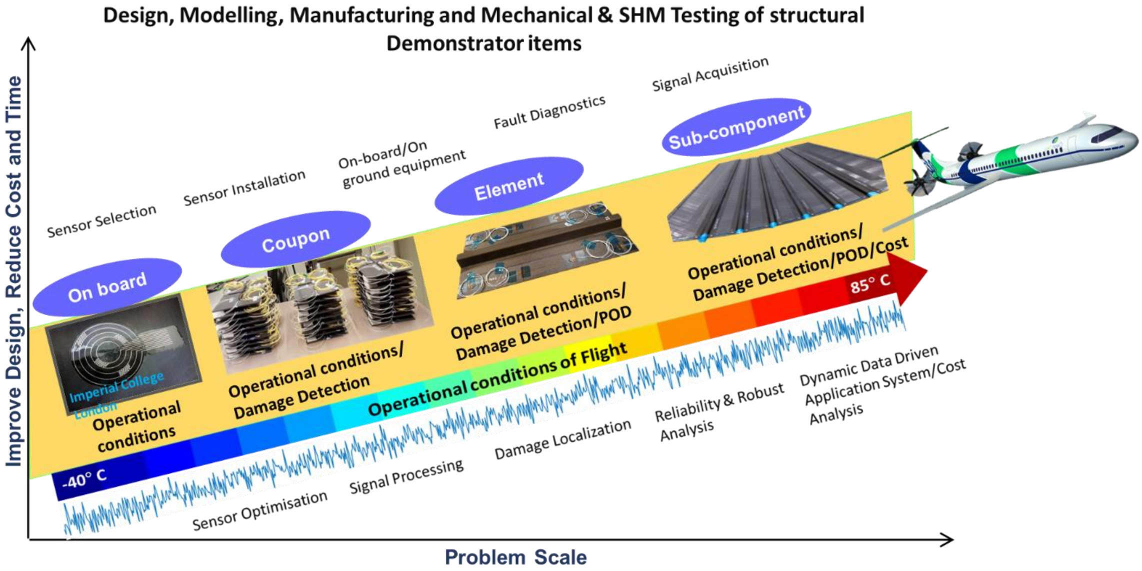

Figure 1: SHM industrialisation roadmap

The project represents the most comprehensive assessment of a complete SHM system to date for composite airframe, covering integrity, durability, and longevity of every piece of equipment and installation on board the aircraft as well as diagnostic and prognostic assessments. Fifteen different transducers incorporated within five key technologies (Ultrasonic Guided Wave; Fibre Optics; Hybrid; Multifunctional Sensors; Magnetostrictive) were tested following the regulations and down selected depending on their performance. Parts (coupon, element, sub-components) were manufactured following a robust and reliability design-based optimisation and tested with and without SHM installed following the industrial building block approach. Advanced diagnostic and prognostic assessment including uncertainty quantification due to operational and environmental conditions provides the first fully integrated SHM technology-methodology system for composites airframe.

Figure 2 shows the results of SHM tests to detect BVID in a 2 m flat composite stiffened panel. Next, three 5 m long curved composite stiffened panel will be sensorized and using a specially developed triaxial mechanical machine tested. Large scale mechanical and SHM testing is complemented with virtual simulations using a massively parallel finite element code.

Several major innovations which include lightweight diagnostic skin (film) with sensors/actuators using inkjet printing, multi-functional sensors for monitoring curing and bonding degradation, have reduced the additional weight burden of SHM by as much as 70% as well as enhancing the industrialisation process. This novel technology was tested with SHERLOC QSP (GAP) where Cetim designed and manufactured thermoplastic window frame bonded to a thermoset skin. QSP technology not only reduced the scrap waste to zero it achieved curing of the parts in less than a minute.

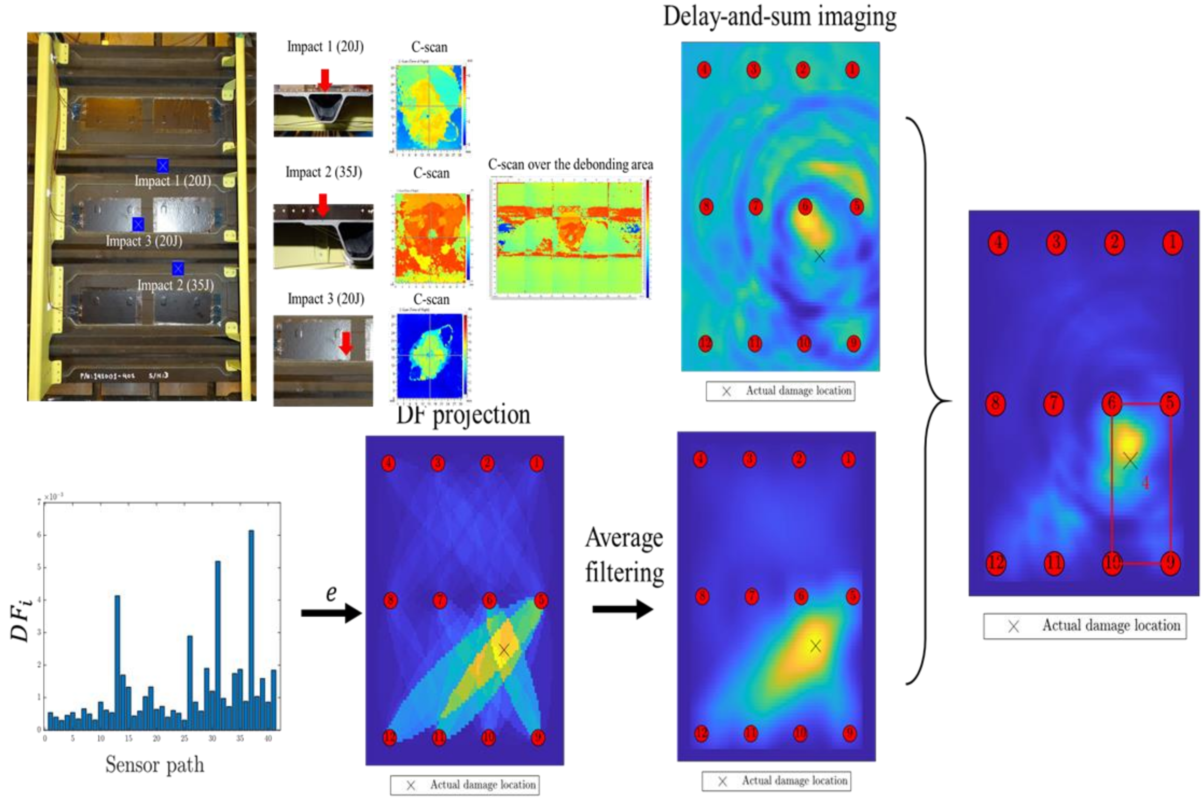

Figure 2: Damage Detection

Together with MASCOT consortium (GPA), a novel multi-level cost model software is being developed were SHERLOC's SHM cost module is being integrated with manufacturing and maintenance cost analysis to quantify the overall benefits of sensor integration for each composite aircraft component. This will directly feed into the more affordable composite fuselage in airframe

SHERLOC's consortium comprises of experts around Europe from both from academia and industry: Imperial College London (Coordinator), Hellenic Aerospace Industry (HAI), Element Materials Technology Seville (ELEMENT), Barcelona Supercomputing Centre (BSC), University of Sheffield (US), Universidad Politécnica de Madrid (UPM), Vrije Universiteit Brussel (VUB), FIDAMC.

7.3 Galvanic Corrosion Sensors

M. Balmond - BAE Systems

7.3.1 Summary

BAE Systems has previously developed and qualified a corrosion sensor that monitors the depletion of the corrosion protection afforded to aluminium alloys by an inhibitor based paint scheme. The sensor is available for specific paint schemes (including Cr and non-Cr inhibitors) and for specific alloys (including 2000 and 7000 series). However, in some circumstances, galvanic corrosion is the predominant mechanism. Consequently, BAES has modified its corrosion sensor capability to include a sensor that can have both an inhibitor based paint coating and galvanic couples incorporated within the sensing elements. This allows a more comprehensive condition monitoring system to be implemented.

7.3.2 Introduction

Corrosion sensors are used on BAE Systems aircraft in order to continuously monitor corrosivity within internal bays that are only normally accessed periodically. The sensors allow corrosion to be detected as soon as it begins rather than when the bay is next opened for inspection.

If corrosion is caught early, the cost of dealing with the issue is generally much less than if corrosion is given the chance to progress. Additionally, by monitoring the rate of corrosion within aircraft bays, maintenance planning becomes possible i.e. appropriate plans for rectification of the issue can be made prior to the next service.

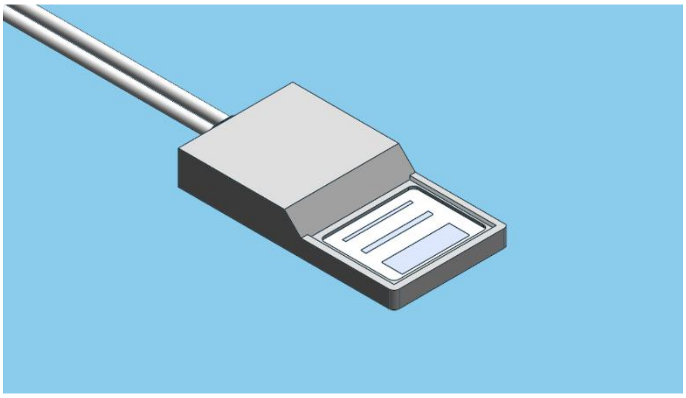

Figure 1: BAE Systems Corrosion Sensor

In certain locations on aircraft, corrosion is accelerated by the presence of dissimilar materials, resulting in the formation of galvanic cells. This is a significant issue when composite structures are attached to alloy structures. Additionally, fasteners made from another material type (e.g. titanium) are typically used to fix the composite to the alloy and this produces more galvanic couples.

7.3.3 Galvanic Sensing

In order to monitor the rates of corrosion due to the presence of galvanic couples within aircraft bays, a variant of the BAE Systems corrosion sensor has now been developed which has galvanic couples incorporated within its sensing elements (patented design). As with the sensors that are routinely fitted to aircraft at present, the new galvanic sensors can also be coated with the paint scheme that is used on the aircraft itself. Such a sensor is referred to as a “smart witness plate” i.e. the sensors are made from the same materials as the aircraft (alloy + galvanic couples + corrosion inhibiting paint coating) in order to provide representative monitoring.

7.3.4 The Smart Witness Plate Approach

Aircraft primers contain corrosion inhibitors which leach out to protect any exposed alloy due to defects (e.g. scratches) in the paint coating. The “smart witness plate” sensor uses the same approach in order to take account of the levels of protection provided by the inhibitors. The sensing elements are positioned beneath “engineered defects” in the coating.

By using engineered defects of three different widths, the sensors are able to monitor the rate of inhibitor degradation for different sized defects. The wider defects provide advance warnings of corrosion (ahead of issues occurring on the aircraft structure itself). If the sensor element beneath the narrowest defect corrodes then this is a warning that the structure in the bay is likely to start corroding too and an inspection of the bay should be carried out before this point is reached – the condition status for every bay, on every aircraft, is presented using a red/amber/green traffic light system.

Large cost savings are possible during normal circumstances where the sensors aren’t detecting any significant levels of corrosion at all within particular bays. Previously, additional inspections had to be introduced on some platforms (at significant cost) to monitor interior bay corrosion due to the length of time between services and the levels of corrosion that were being uncovered when services were carried out. The sensors allow a shift towards condition based maintenance instead of having to open up bays more frequently for such costly additional inspections.

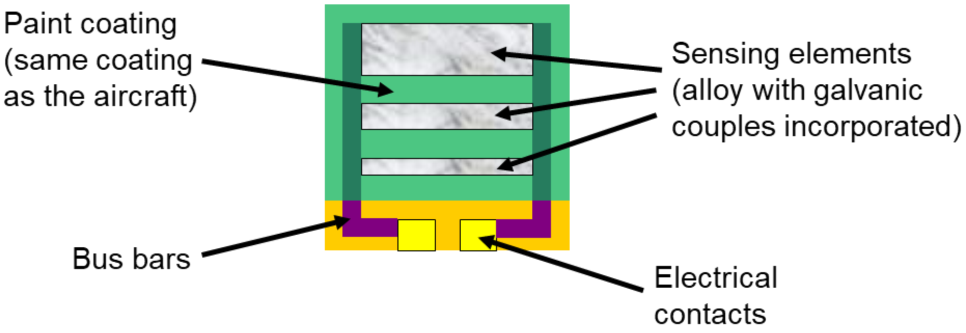

Figure 2: Smart Witness Plate Corrosion Sensor Diagram

Sensor function is evaluated by testing alongside actual pieces of aircraft material (test plates) in salt spray chambers. The sensor outputs are monitored throughout testing in order to ensure that their outputs are representative of the rate of corrosion of the neighbouring test plates. The galvanic sensors routinely show an enhanced rate of corrosion during salt spray testing compared with the traditional (non-galvanic) sensors and test plates.

7.3.5 Conclusions

Sensors have been successfully developed with galvanic couples incorporated within the sensing elements.

The addition of galvanic sensing capability routinely results in faster output response times from the sensors in the salt spray test environment, in the way that would be expected, due to the enhanced rate of corrosion caused by the presence of the galvanic couples.

The galvanic sensors can still be configured as “smart witness plate” type sensors, coated with the same paint scheme as the aircraft, hence the effect of the corrosion inhibitors in the paint coating can still monitored in addition to monitoring the effect of the presence of galvanic couples.

7.3.6 Future Work

The standard sensors, which are currently being installed on aircraft, were tested alongside test plates in several different environments prior to establishing that their outputs were representative over a wide range of different corrosivities i.e. salt spray testing is an accelerated test with a corrosivity that is much higher than many environments that a sensor may actually be subjected to during service. Testing the galvanic sensor function alongside test plates in a range of environments (in the same way that this was originally done for the standard sensors) would enable assessment of function in lower corrosivity environments.

8 Advanced repair and coating technologies

8.1 Optimal Control of Resin Injection Repair for Composite Laminates

A. Asiliskender - Imperial College London

The main objective of this work is to improve the efficiency and reliability of resin injection repair used on composite structures. This is achieved by developing novel methods to quantitatively assess and optimise the resin injection process through modelling and simulation. The method strategy is to; reconstruct damage geometries, simulate resin flow virtually and finally iterate inlet/outlet configurations in order maximise the fill efficiency.

An extensive literature review of resin injection repair is being compiled in collaboration with Queen's University Belfast (QUB). The literature review includes the following topics: composite damage types suitable for resin injection; resin classes that may be considered for resin injection repair; nanomodification of repair resins; imaging and scanning of damaged composites; modelling of damage for resin injection (including both Finite Element Analysis (FEA) and Computational Fluid Dynamics (CFD) modelling).

One of the research tasks is to digitally reconstruct damage geometries in 3D using Computed Tomography (CT) scanning techniques, in order to create a high detail, high fidelity 'gold standard' simulation to compare against experimental data. The equipment and computing power requirements of such a technique are difficult to obtain and, while feasible in this study, they are not currently practical in the field. The validation of the physics models to be used for this high-fidelity simulation is under progress. A 3D geometry of a damaged composite specimen has been reconstructed (Figure 1) with a view to prepare it for a CFD injection simulation.

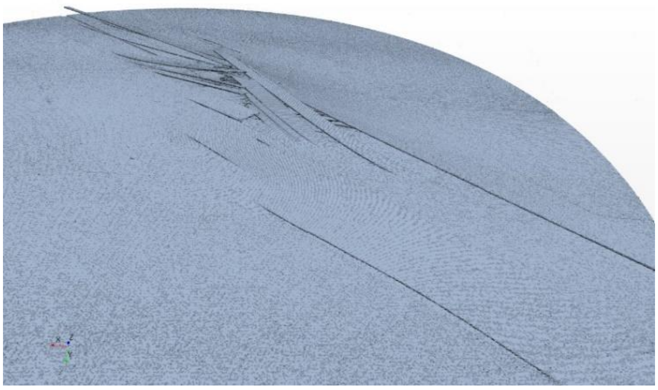

Figure 1: A 3D reconstruction of a damage composite specimen from X-CT data.

Due to impracticality and high cost of 3D reconstruction and simulation in the near future, a two-dimensional reduced order method is proposed which drastically reduces the cost of reconstruction and simulation. Such a method works by assessing the damage on a composite (e.g. Figure 2) from a top-down 2D perspective using Ultrasonic C-scan technique, then applying a porosity field to represent the damage (Figure 3), which itself is assessed by the changes in a composite specimen's thickness before and after damage using ultrasonic testing.

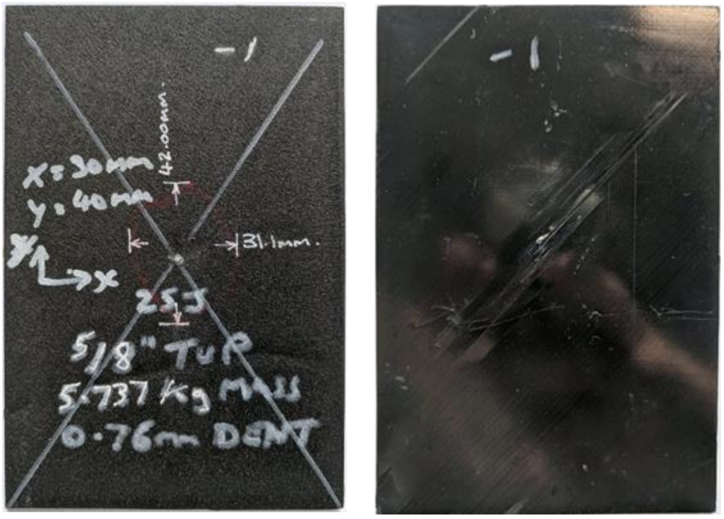

Figure 2: Composite specimen (provided by QUB), left – front, right – back

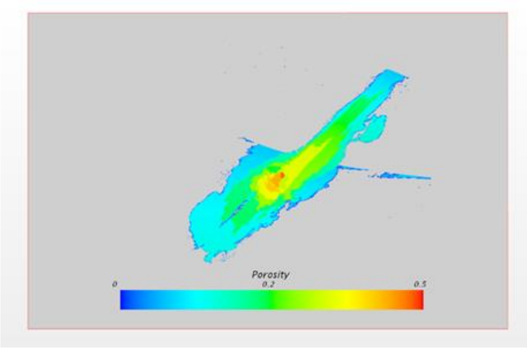

Figure 3: Filtered porosity map

Figure 4: 2D reconstruction

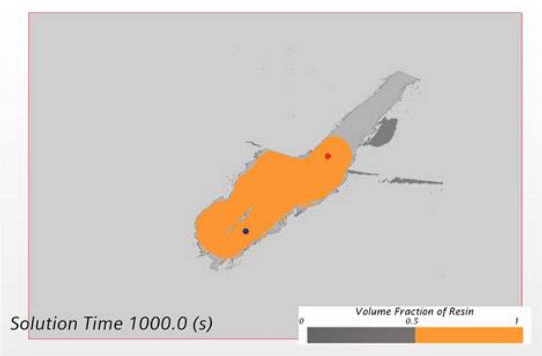

Figure 5: Reduced-order method simulation result of one of the cases, red and blue dots indicate injection port and outlet vent respectively.

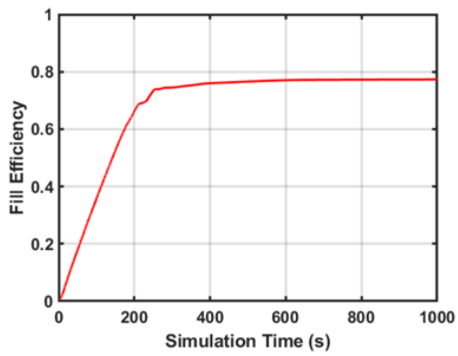

Figure 6: Filling efficiency over injection simulation time

The porosity field is applied to a constitutive equation in order to create a permeability field for use directly in the porous flow physics model (Darcy's Law). The physics models used for this simulation have been validated by using experimental or theoretical results from literature or through derived analytical solutions of the case at hand. Additionally, a reconstruction of a damaged composite specimen (Figure 4) provided by QUB (Figure 2) has been completed and simulations of various repair configurations has been undertaken in order to assess efficacy of these configuration behaviours by analysing the ratio of volume filled by resin as well as the structure of the filling (Figures 5 and 6). A paper is being prepared with further details of the 2D reduced-order method.

A sensitivity study on a nanomodified resin for repair will be conducted. The changing rheology with increasing nanofiller loading, its effect on the CFD damage filling results and its ultimate effect on the repair effectiveness when used on a damage geometry will be evaluated.

The modelling work will be verified by using both a mock-up geometry and impact test panels. The purpose of the mock-up geometry is to allow the assessment of the proposed 2D reductive methodology together with a constitutive equation in a representative case and potentially compare the flow from this mock-up to its digital 3D version. Impact test panels have been produced and damaged by QUB. These will be simulated using the 2D method in order to provide guidance for the repair procedure, which is aimed to be compared to the unguided procedure for changes in infiltration efficacy and compression after impact strength testing.

The proposed 2D reduced-order method uses existing and practical non-destructive evaluation techniques and could potentially increase the efficiency and reliability of injection repairs in the field. Moreover, the models developed within this project could be used to assess alternative resin types and nanofillers for improved injection repair. Finally, this research project initiates avenues for optimising the overall reconstruction, simulation and injection strategy.

The author would like to thank Dstl for the funding received for this project through the Materials for Strategic Advantage (MSA) Programme.

8.2 De-icing using icephobic coatings alongside thermal de-icing systems

J. Brierley - University of Nottingham

Helicopter blade icing is a serious safety concern with icing on the leading-edge reducing lift, increasing drag and reducing the stall angle. Thermal de-icing systems are a vital safety system; coatings could provide a sacrificial layer to erosion while reducing ice adhesion strength and the lifetime energy consumption of the active system to form a hybrid solution.

Icephobic coating has the capability of minimising and delaying the ice accretion on the aircraft surface and lowering the ice adhesion strength to facilitate ice removal. Applying icephobic coatings on component surfaces has attracted more and more attention in the aerospace and wind energy sectors. Icephobic coating is a low-cost and high-efficiency approach, and the coating can be used on its own, or to be integrated with an active ice protection system. The research group at the University of Nottingham has developed various types of icephobic coatings, which demonstrate impressive icephobicity, durability, and erosion resistance.

The aims of this research are to:

1. Consider an intermediate, hybrid solution of an electro-thermal de-icing system enhanced by an icephobic coating.
2. Consider what a coating with this primary function should do, and the differences when compared to a passive solution where a coating is capable of functioning alone.
3. Study the heat transfer and fluid mechanics of blade icing, to allow specific characterisation of a coating's performance.

Many icephobic coatings that have a low ice adhesion strength are very fragile, for example, slippery liquid infused porous surface (SLIPS) that rely on a porous structure often filled with a hydrophobic oil. Some sacrifices in this aspect of performance are expected in order to improve durability.

This research assumes that a passive solution (standalone coating) is unlikely to be found when active solutions can be designed out, and the most likely scenario is that successful coatings will be applied retroactively. This is particularly obvious when considering that commercial fixed-wing aircraft have a typical lifespan of 25 to 30 years.

This research concerns how coatings can work alongside active systems, which is often not considered. Since material is being added between the heater and the ice, that can often be insulating. Consequently, it is likely for many reasonably thick coatings (consider 50 or 100 μm) that without additional loading, there will be an additional energy cost for thermal de-icing in a single cycle. So, it is crucial to design coatings to reduce this cost and mitigate it by considering the lifetime associated cost or cost across a single flight and how coatings can reduce that. Coatings can reduce the frequency of icing by delaying its formation, limiting the maximum accretion by having a low ice adhesion strength and providing a sacrificial layer to extend the lifespan of a blade or wing. Overall, making the de-icing system safer and more efficient.

To conclude, it is important to design an icephobic coating for its specific application; changing one property of the coating may have conflicted effects across different criteria of the performance. A hybrid solution could provide a better solution, compared with a completely passive solution of a standalone icephobic coating. Durable icephobic coatings offer the potential for improved flight safety and performance by improving the efficiency of electro-thermal de-icing systems.

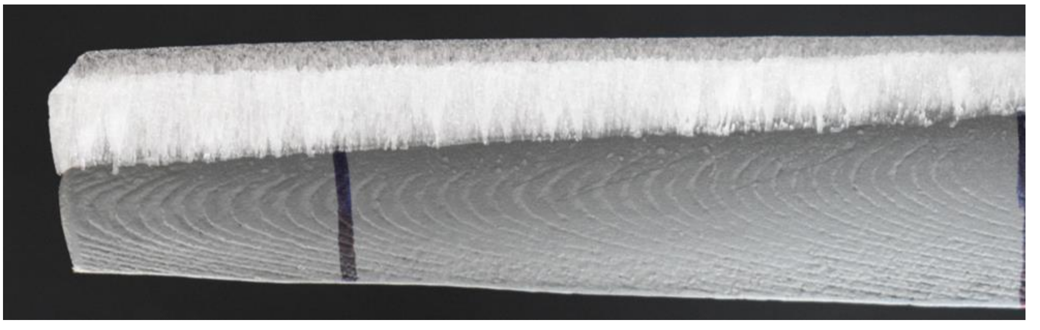

Figure 1 - Preliminary image from a blade icing experiment formed in a cloud and environmental chamber.

The Surface Engineering Group within Advanced Materials Research Group (AMRG) at the University of Nottingham has the expertise to address surface and interface issues from multi-disciplinary points, covering both fundamentals and engineering applications. The research objectives range from surface and interface design in atomic and molecular level, to film/coating fabrication for the functionalisation and protection of engineering components, as well as the related microstructural analysis and coating performance evaluation in aggressive environments. The group has the capabilities to provide surface/interface engineering solutions for various industrial sectors, such as aerospace, energy, automotive, and healthcare, etc., and state-of-the-art facilities are available to meet the different requirements. For more details, please contact Dr. Xianghui Hou Xianghui.hou@nottingham.ac.uk.

9 Advanced composite materials and structural design approaches

9.1 Multi-functional Shape Memory Alloy Tufted Composite Joints

F. Ciampa - University of Surrey

Structural fibre reinforced plastic (FRP) composite joints are widely used in land vehicles, naval ships, unmanned vehicles, military aircraft and weapons. However, the greatest technical challenge to enable the increased efficiency of FRP composites is to develop structural joining solutions that are (i) mass efficient, (ii) robust and certifiable, and (iii) supportable in-service and through life with minimal inspection and maintenance costs. The “holy grail” of composite joints is to combine multiple features including damage resistance, damage tolerance, self-repair, in-service health monitoring and ease of inspection.

The Multi-functional Shape Memory Alloy Tufted Composite Joints (MuST) project between University of Surrey (Lead), QinetiQ UK and the UK National Composite Centre directly addresses this challenge through the Defence and Security Accelerator (DASA) call “*A Joint Effort – Integrating Advanced Materials onto Military Platforms – Challenge 1, Integration of Composites*”. The initial Phase 1 project aimed to deliver the proof-of-concept for a ground-breaking multifunctional composite joining system that can benefit military structures in all domains by enhancing damage tolerance whilst also enabling, for the first time, both “self-repair” and “self-sensing” capabilities. The proposed composite joint was manufactured by tufting shape memory alloy (SMA) wires into dry carbon fabric preforms prior to resin infusion. Tufting is a cost-effective manufacturing process that uses commercially available automated systems to insert the yarn through-the-thickness of a laid-up dry fabric composite. Unlike stitching, tufting uses a single needle and requires access only from a single side of the preform, thus considerably simplifying the manufacturing complexity of the joint. Mechanical testing carried out in Phase 1 demonstrated that the “superelastic” property of tufted SMA wires enabled higher ultimate strength and toughness of the joint, whereas the “shape memory” effect of SMA tufts was used to initiate local “self-repair” via crack bridging and crack closure, thus delaying/preventing growth of delamination or disbonds. Moreover, the electrical resistance changes and the resistive heating provided by SMA wires successfully enabled in-service strain monitoring and rapid crack visualisation via thermography. Figure 1 shows a close-up of the SMA tufted composite fabricated in Phase 1.

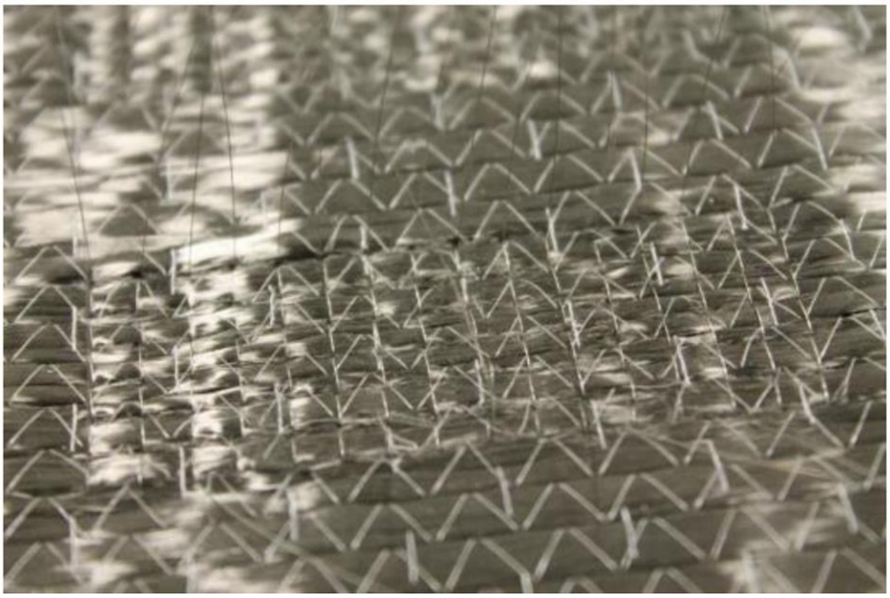

Figure 1 - A close-up of the SMA tufted composite.

The Phase 2 project proposal is currently undergoing and builds on the Phase 1 project. It aims at further optimising the design and manufacturing of SMA carbon fibre/epoxy composite joints. This project will involve the physical testing and experimental analysis of composite T-joints reinforced with tufted SMA wires. Phase 2 will focus on the multi-functional capabilities of the composite T-joint and the optimisation of its tufting design parameters. SMA tufted T-joints will provide much higher ultimate strength and strain energy absorption than current composite joint technology. In addition, tufted SMA wires will provide the unique capability of closing cracks when activated, thus increasing durability. Finally, the electrical resistance changes and the internal low-power resistive heating provided by SMA wires will enable, for the first time, in-service strain monitoring of T-joints and damage visualisation via thermography. Similarly to Phase 1, the UK project will be enhanced by continuing the established collaboration with the Australian SBIRD consortium consisting of QinetiQ Australia and the RMIT University of Melbourne, who are developing numerical modelling techniques to aid with understanding and optimisation of the proposed joining system.

Further details on the above work can be found at F. Ciampa *et. al*., Compos. A. Appl Sci Manuf, 147 (2021)
https://www.sciencedirect.com/science/article/pii/S1359835X21001779

9.2 Advanced Design of Composite Structures for Future Combat Aircraft

P. Hopgood, D. Hallam - Defence Science and Technology Laboratory (Dstl)

The National Composites Centre (NCC) and Dstl have joined forces to facilitate innovative R&D in combat aircraft composite structures. This exciting new partnership will explore the art of the possible for composite structures of future combat aircraft. The emphasis is on engaging the wider community to explore revolutionary design and innovative technologies, reducing mass and through-life cost, and increasing performance, availability, adaptability and modularity. This ranges from innovative approaches to overall structural-layout, manufacturing and assembly to the optimal combination of detail features and material selection.

There are two primary aims:

- To develop airframe design concepts through trades studies and worked examples, and

- To systematically collate and develop underpinning data upon which the airframe design trades are built, including the performance of composite materials and features, and to identify and mitigate those features that are constraining performance and cost

The project will identify the scope for transformational design, and will develop a tree of design options.

Dstl would like this project systematically to identify those features and failure modes that are constraining designs, and to explore novel and/or radical approaches to the elimination or mitigation of the limiting features and failure modes. This is clearly a challenge. The project will explore whether this is achievable through combinations of: platform-level configuration, structural layout, structural design philosophy, feature elimination, failure mitigation and material selection for example. Priority will be given to transformational ideas.

Indicative interests include: High-strain repairs; Reduced through-life structural-integrity risk; Rapid, low-cost qualification; High-strain features; Crack-arrest features; Alternative materials; High damage-resistance and damage-tolerance; Fatigue insensitivity; Low-risk structures; Robust design; Reduced qualification burden; Material interchangeability...

Further information is available via the links below.

https://www.nccuk.com/media/pedgwrlq/adcosca_guidance.pdf
https://www.nccuk.com/sectors/aerospace-defence-and-space/combat-aircraft/
https://www.gov.uk/government/news/ncc-and-dstl-seek-innovation-in-composite-structures-for-combat-aircraft

Initial distribution

1. Dstl KIS Athena
2. Contributors
3. ICAF National Delegates

Report documentation page

v5.0

* Denotes a mandatory field

1a.	**Report number: *** DSTL/TR132845	**1b.**	**Version number:** v1
2	**Date of publication: *** 30/06/2021	**3.**	**Number of pages:** iiiiii + 52
4a.	**Report UK protective marking: ***		OFFICIAL
4b.	**Report national caveats: ***		NONE
4c.	**Report descriptor: ***		NONE
5a.	**Title: *** Review of aeronautical fatigue and structural integrity investigations in the UK during the period April 2019 - April 2021		
5b.	**Title UK protective marking: ***		OFFICIAL
5c.	**Title national caveats: ***		NONE
5d.	**Title descriptor: ***		NONE
6.	**Authors: *** Hallam, D.		
7a.	**Abstract: *** This review is a summary of the aeronautical fatigue and structural integrity investigations carried out in the United Kingdon during the period April 2019 to April 2021. This review has been compiled for the International Committee on Aeronautical Fatigue and Structural Integrity (ICAF) 2021 website (www.icaf.aero.com) and the 2021 ICAF webinar. The contributions generously provided by colleagues from within the aerospace industry and universities are gratefully acknowledged. The names of contributions and their affiliation are shown below the title of each item.		
7b.	**Abstract UK protective marking: ***		OFFICIAL
7c.	**Abstract national caveats: ***		NONE
7d.	**Abstract descriptor: ***		NONE
8.	**Keywords:** Aeronautical fatigue, Structural integrity, ICAF		

Please note: Unclassified, Restricted and Confidential markings can only be used where the report is prepared on behalf of an international defence organisation and the appropriate prefix (e.g. NATO) included in the marking.

* Denotes a mandatory field

9. Name and address of publisher: * Dstl Platform Systems Porton Down Salisbury Wilts SP4 0JQ	**10. Name and address of funding source:**
11. Funding source contract:	
12. Dstl project number:	
13. Programme:	
14. Other report numbers:	
15a. Contract start date:	**15b. Contract end date:**
16. IP conditions for report: *	Non-MOD Funded Dstl authored report
17a. Patents:	YES
17b. Application number:	No
18. Release authority role:	

Guidance on completing the report documentation page can be found on the Gov.UK website.

THIS PAGE INTENTIONALLY LEFT BLANK

Ministry of Defence